https://doi.org/10.5194/egusphere-2024-2258
Preprint. Discussion started: 31 July 2024

Coupled water-carbon modelling in data-limited sites: a new approach to explore future agroforestry scenarios

Salim Goudarzi*[1], Chris Soulsby[1], Jo Smith[2], Jamie Lee Stevenson[1], Alessandro Gimona[3], Scot Ramsay[3], Alison Hester[3], Iris Aalto[4], and Josie Geris[1]

[1]School of Geosciences, University of Aberdeen, UK
[2]School of Biological Sciences, University of Aberdeen, UK
[3]The James Hutton Institute, Scotland, UK
[4]Department of Geosciences and Geography, University of Helsinki, Finland

Submitted: 19/07/2024

Abstract

Agroforestry is considered an important strategy for mitigating against, and adapting to, climate change. Questions yet remain regarding the potential impacts of different tree species on water/carbon cycling at different locations, scales and under different climatic conditions. There is an urgent need for numerical models capable of quantifying agroforestry impacts on a host ecosystem services including carbon sequestration and soil water/river flow regulation. A key challenge in modelling agroforestry systems is that they depend heavily on soil moisture as the main driver of many biogeochemical processes. Soil moisture itself is highly variable with soil properties (and therefore with location) but also with depth. Given that target sites for agroforestry are often ungauged, location-specific agroforestry modelling must inevitably rely only on data available from satellites and/or nearby weather stations which do not typically cover the subsurface, i.e., there is an incommensurability between data-availability and system complexity. To overcome this, we propose RSEEP, a new ecohydrological model that only requires rainfall, potential evapotranspiration, and surface soil moisture for its calibration. We demonstrate RSEEP's capability in water cycling for a site in Scotland where soil moisture observations are available for different depths and vegetation types. We then couple RSEEP to the well-known RothC soil carbon model to (i) test RothC's sensitivity to water cycling method, and to (ii) simulate water-carbon dynamics of three different silvo-pastoral agroforestry systems (all at 400 stems/ha density) in Scotland; these systems are: with evergreen conifer (Scots Pine), deciduous conifer (Hybrid Larch), and deciduous broadleaf (Sycamore) trees. We find that not including more accurate soil moisture accounting methods in RothC can significantly overestimate soil carbon stocks. Under the current future climate pathway (RCP6.0), 40 years after planting trees, above+below ground carbon storage can be 2-5 times (100-250 t/ha) higher under silvo-pasture than under pasture depending on species, with Larch having the highest potential and Sycamore the lowest. Larch also exhibits the highest potential for preserving soil moisture under drier conditions, but Pine shows the highest potential for river flow regulation under both wet and dry conditions at our site. The choice of species is therefore important and should be made site-specifically and based on the ecosystem service and management priorities/objectives. Examining our scenarios under drought- and flood-relevant conditions and scales is a logical next step.

1 Introduction

Climate change mitigation polices typically revolve around reducing carbon emissions and increasing its sequestration, while climate change adaptation policies tend to focus on increasing land productivity under the

*Correspondence: Salim Goudarzi (salim_ goodarzi@yahoo.com)

https://doi.org/10.5194/egusphere-2024-2258
Preprint. Discussion started: 31 July 2024

expected adverse future temperature and precipitation patterns (e.g., IPCC 2023). However, the two agendas overlap significantly because carbon and water cycles are closely linked (Gentine et al., 2019). Agroforestry, the practice of growing trees/shrubs in association with crops/pasture and/or livestock (Nair et al., 2021), can provide many benefits including carbon sequestration and soil water regulation (Smith et al., 2013). This is why agroforestry is recognised as a potential solution to help meaningfully, and simultaneously approach mitigation and adaptation (Noordwijk et al., 2011, Duguma al., 2014a,b).

While more common in tropical latitudes, agroforestry practices are yet to be widely adopted in regions with temperate, humid climates (Smith et al., 2013, Den Herderet al., 2017, Garcia de Jalon et al., 2018, Sollen-Norrlin et al., 2020), e.g., Scotland. The barriers to wider adoption typically fall within one of three categories; a lack of (i) adequate policies to promote and enable agroforestry (Mosquera-Losada et al., 2018), (ii) practical skills in establishing/maintaining trees, or awareness of their potential economic benefits (Abdul-Salam al., 2022), and (iii) sufficient evidence of effectiveness (Smith et al., 2012). The latter is partly due to the time/cost associated with pilot agroforestry experiments resulting in very few examples being yet available of complete cycles of systems through to tree harvest (Smith et al., 2012), and partly due to the complexities inherent in tree-soil-atmospheric systems (Menichetti et al., 2020) making them difficult to assess using numerical models, which in turn poses as a barrier to reporting agroforestry's contribution to climate policies (Hübner al., 2021, Cardinael al., 2021).

One of the reasons for the difficulty in modelling agroforestry is the presence of trees and their interaction with soil moisture. It is generally accepted that most trees have the ability to shift their water source from shallow to deeper layers under drier conditions Liste & White 2008, Dawson 1996, 1993, Emerman & Dawson 1996, Caldwell & Richards 1989. For systems involving trees, this makes it particularly important to estimate soil moisture and root water uptake at different depths (see, e.g., Smith et al. 2021). This importance is further accentuated when considering climate change and that the tendency of soils to store and emit carbon strongly depends on soil moisture (amongst other factors, Falloon & Betts 2010, Falloon et al. 2011, Gottschalk et al. 2012, Moyano et al. 2012, Jebari et al. 2021). For these reasons, part of our focus here is on how to estimate soil moisture at different depths in a simple, parsimonious manner, while the other part is on exploring agroforestry impacts on water and carbon. On an aside, note that profile soil moisture estimation is an old problem in hydrology that goes back decades (Liu & Yang, 2022). In fact, soil moisture has been described as the most challenging variable to estimate (Mishra et al., 2020), so while we are motivated by its particular importance in agroforestry systems, our parsimonious approach to estimating soil moisture is likely to be of interest in other applications.

The difficulty in modelling soil moisture stems mainly from a lack of data to constrain the additional parameters that would be needed to develop a depth-dependent model of the soil (i.e., not from inadequate understanding of the physical processes themselves Li et al. 2023). Today, satellite datasets are readily available to force, calibrate, and validate (eco)hydrological models in the top 5-10 cm layer of the soil, but similar below-ground datasets are limited to sparse, point-measurements often at sites that are not suitable/targets for the intended application (Li et al., 2021, Duethmann al., 2022, Wang et al., 2023). This makes reliable, location-specific predictions a real challenge. To boost temperate agroforestry uptake, we would argue that location-specific predictions are essential to help stakeholders in their decision making.

To this end, we developed RSEEP, a simple, parsimonious, conceptual ecohydrological model to **R**etrieve **S**oil-moisture and **E**stimate **E**cohydrological **P**artitioning. RSEEP is a three-parameter model that encompasses the main soil-tree-atmospheric interactions but only requires rainfall, potential evapotranspiration and surface soil moisture information for its calibration. In a data-rich site in Scotland where detailed profile soil moisture observations are available, we show RSEEP's strengths and weaknesses in estimating profile soil moisture. In a nearby data-limited pilot agroforestry site, where soil moisture observation is limited to the top of the soil profile, we then couple RSEEP with the widely used RothC soil carbon model, and used the coupled model to: (i) examine the impact of a different soil moisture accounting procedure on RothC's carbon storage/emission estimates; and (ii) quantify the impacts of different agroforestry scenarios in North East Scotland and under the current future climate projection pathway (RCP6, until to 2080).

https://doi.org/10.5194/egusphere-2024-2258
Preprint. Discussion started: 31 July 2024

2 Study sites

Our study considers two separate sites as shown in Figure 1: the pilot agroforestry experimental site in Glensaugh, Scotland, and the Cruickshank Botanic Garden located in Aberdeen, Scotland. Cruickshank Botanic Garden is a data-rich site in terms of soil moisture data availability at different depths, so it is used here to test and highlight the strengths and weaknesses of our proposed model (RSEEP) in retrieving profile soil moisture. The agroforestry site at Glensaugh, is a data-limited site with regard to soil-moisture information because datasets cover only the near-surface (i.e., 6 cm depth) zone. However, Glensaugh also provides before/after (agroforestry) soil carbon/biomass datasets. Thus, by coupling RSEEP with RothC (a soil carbon model, will be introduced in section 3.2.1) in this data-limited site we aim explore an agroforestry scenario.

2.1 Cruickshank Botanic Garden

Cruickshank Botanic Garden is owned by the University of Aberdeen, located in North East Scotland. Geologically, the bedrock in the area is composed of metamorphic psammite and semipelite, in contact with the Aberdeen granite to the West and conglomerates and sandstones to the East. The bedrock is overlain by glacial till, sands and gravel deposits. Soils are typically mineral podzols and brown soils. The climate of Aberdeen is temperate/boreal oceanic with average precipitation of 850 mm/yr. Monthly mean temperatures range from 3 ^{o}C in January to 14 ^{o}C in July/August (Stevenson et al., 2023). Ecohydrological monitoring began in December 2020 and involved soil moisture measurement at five different depths (namely 10cm, 20cm, 40cm, 60cm, and 100cm below the surface) and under three different species: evergreen conifer (*Abies korena*; 30 years old and 6 m tall), larger deciduous tree (*Fagus sylvatica*; 60 years old and 10 m tall), and grassland site, which contained a variety of species associated with this habitat, such as *Taraxacum spp.*, to a height of ca. 0.4 m. The three sites had similar soil properties being an undifferentiated silty-clay-loam subsoil, with distinct organic-rich topsoil. Following Stevenson et al. (2023), evergreen conifer is assumed to have a time invariant Leaf Area Index (L_{AL}) value of 7 m^2/m^2. For the time-variant canopies, a trapezoidal shape was employed, in the absence of repeated L_{AL} measurements. The timing of rises, peaks and decreases of this trapezoid were directly guided by field observations and sapflux measurements where available, resulting in an initial value on 1st March of 1.5 m^2/m^2 for the larger deciduous tree which remained constant before rising to 6 m^2/m^2 between 12th May and 17th July. The grassland timeseries followed the same temporal pattern but rose from 1.5 to 4.

2.2 The Glensaugh agroforestry experiment

Glensaugh is a 1100 ha research farm owned and operated by the James Hutton Institute and is located ∼56 km south West of Aberdeen, Scotland. The farm contains an experimental agroforestry site. The silvopasture experiment was established on permanent improved grazed pasture in spring of 1988. It is composed of three main blocks, A, B and C (see Figure 1 b). Three species of trees were planted in 1988 and replicated in each block, at 100, 200, 400, and 2500 stems/ha densities. However, we only consider the 400 stems/ha case in this study. Species are: (1) Deciduous broadleaf (*Acer pseudoplantanus*, or Sycamore), (2) Deciduous conifer (*Larix eurolepis*, or Hybrid Larch, hereafter referred to as Larch), and (3) Evergreen conifer (*Pinus sylvestris*, or Scots Pine, hereafter referred to as Pine). Also, separately on each block, an open patch of grazed pasture covered primarily with lolium perenne, or rye grass (hereafter referred to as Grass) is monitored as control.

All plots are grazed from April to October by sheep and, since 2010, occasionally by cattle (Chandler et al., 2018). The understory of the Pine and Grass plots are covered with pasture. In the Larch plots, much of the understorty is covered by a dense litter layer, but the plots are still used by sheep/cattle for shelter. The understory in the Sycamore plots are characterised by patches of bare ground and litter that vary in extent seasonally (Beckert et al., 2015, Chandler et al., 2018). Altitude across the site ranges from 140 m to 205 m. Mean annual rainfall and temperature at Glensaugh are 1168 mm and 8 ^{o}C, respectively (Chandler et al., 2018). The soils at the site are freely drained cultivated humus-iron podzols and brown earths (Beckert et al., 2015) developed primarily on glacial drifts. Median sand content is: 76%, 75%, 69% and 76%; silt: 20%, 21%, 24% and 21%; and clay: 4%, 4%, 7% and 3%, for Grass, Pine, Larch and Sycamore, respectively.

https://doi.org/10.5194/egusphere-2024-2258
Preprint. Discussion started: 31 July 2024

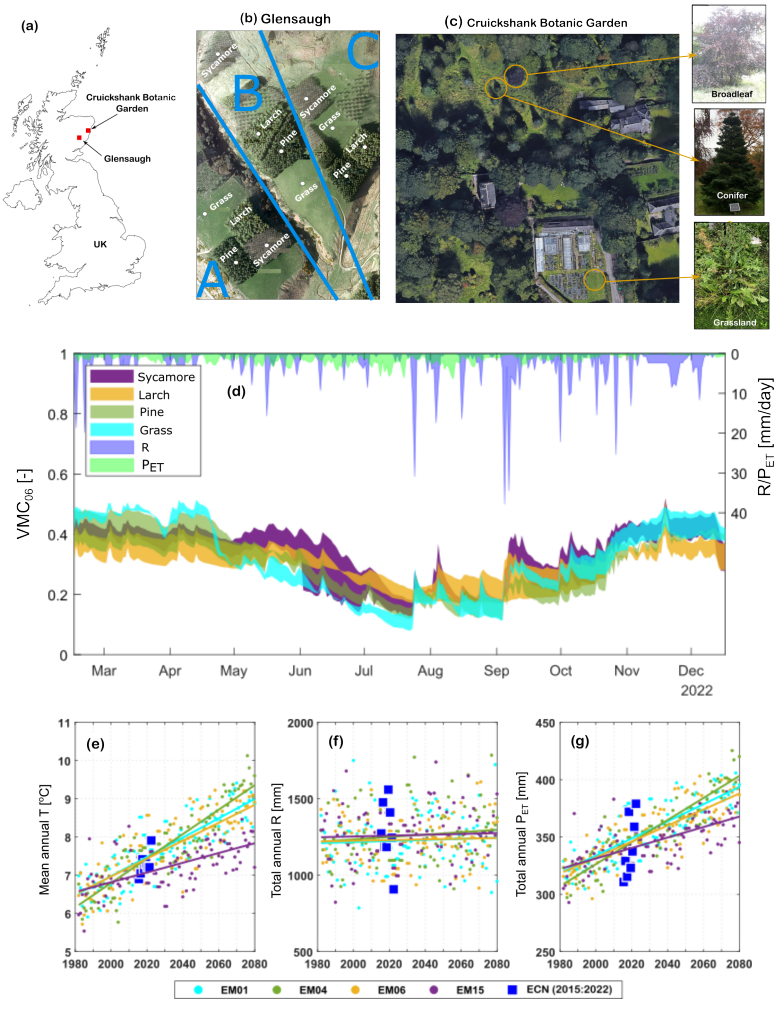

Figure 1: Our two study sites: (a) location of the sites. (b) Glensaugh pilot agroforestry experiment. (c) Botanic Garden is used to test the soil-moisture retrieval performance of RSEEP. (d) Volumetric moisture content at the 6cm depth (VMC_{06}) for each species at Glensaugh; shaded bands show the variation between the different blocks (A, B, and C in panel b). (e-f) CHESS-SCAPE dataset showing the current future climate trajectory (RCP6.0) at Glensaugh.

Soil carbon measurements are available on each plot (i.e., species-block combination) in 2012 (=24 years after trees were planted). To control for inter-plot differences (in e.g., topography, slope, aspect, soil texture, organic content, etc.), for each species we only consider the average value of soil carbon across the three blocks (see Table 1). Soil carbon was also measured on multiple points across the site in 1987 (i.e., before trees were planted). Since no trees were present in 1987, we use the average value across the entire site to represent the conditions before the experiment for all scenarios (see Table 1). But since the details of the management practice is unavailable, we calculate the impact of planting trees on pasture relative to the pasture base-case, to control for unknown effects (more details in section 3.2.4). For the tree sites, plot-average Diameter at Breast Height

https://doi.org/10.5194/egusphere-2024-2258
Preprint. Discussion started: 31 July 2024

(D_{BH}, breast height = 1.3 meters) was recorded in 2012 (Beckert et al., 2015). Also, the year in which each species reached the height of 1.3m (on average) was recorded between 1992-1994 (Nwaigbo, 1996), which is also shown in Table 1.

Table 1: Average soil carbon ($\overline{C}$) and biomass measurements at Glensaugh. $\overline{D}_{BH}$=average Diameter at Breast Height.

Species	$\overline{C}$ *in* 1987	$\overline{C}$ *in* 2012	$\overline{Height}$ *reaching* 1.3*m*	$\overline{D}_{BH}$ *in* 2012
Grass	52 tC/ha	67 tC/ha	-	-
Sycamore	52 tC/ha	74 tC/ha	1993	24.5 cm
Pine	52 tC/ha	78 tC/ha	1994	36.22 cm
Larch	52 tC/ha	81 tC/ha	1992	38.45 cm

Within each plot, hourly volumetric moisture content at the 6cm depth (VMC_{06}) is recorded between January-December 2022, which is subsequently converted to daily timesteps (see Figure 1 d). There is no soil moisture information available for deeper layers. Note that similar to soil carbon data, when calibrating our model (RSEEP, will be introduced in section 3.1.1), we use the soil moisture timeseries averaged across the three blocks to account for inter-block variability. Local climate data are available between 2015-2022 from the Environmental Change Network (ECN) weather station located a few hundred meters from the agroforestry site. For predictions after 2022, and before 2015, we use the CHESS-SCAPE dataset (Robinson et al., 2023) which provides high-resolution (1km-scale) projections between 1980-2080 of multiple climate scenarios for the United Kingdom. We only consider the current trajectory, i.e., the RCP6.0 for the 1-km tile in which Glensaugh is located (RCP=representative concentration pathway, and the number refers to the resulting radiative forcing by the end of the 21st century in watts per square metre). CHESS-SCAPE provides four different parameterisations (EM01:04, see Figure 1 e-g). We utilise all four in our study as a measure of climate data uncertainty. Finally, to correct for biases in the data we multiply the rainfall (R), temperature (T) and Penamn-Monteith potential evapotranspiration (P_{ET}) timeseries obtained from CHESS-SCAPE by appropriate correction factors (which are equal to average of ECN values between 2015-2022, divided by the average CHESS-SCAPE data for the same period). These correction coefficients were 1.13, 0.89, and 0.85, for rainfall, temperature and Penman-Monteith potential evapotranspiration, respectively.

3 Methods

3.1 Soil moisture retrieval for ecohydrological modelling

In the past, various techniques of different complexities have been used to retrieve profile soil moisture from the available data, e.g., statistical (Kostov & Jackson, 1993, Srivastava et al., 1997), physically-based (van Dam & Feddes, 2000, Sadeghi et al., 2016), empirical (Srivastava et al., 1997), neural networks (Pan et al., 2017), wavelet transform (Qin et al., 2018). While the choice of model has been partly influenced by application, it has been mainly constrained by data availability. For large-scale applications in particular, parsimonious methods requiring fewer inputs are logically preferred. Among such methods, the exponential filter (EF) (e.g., Tobin et al. 2017), and the principle of maximum entropy (POME) (e.g., Singh 2010) have generated the most interest in recent years (Mishra et al., 2020). Between the two models, POME tends to have a better overall performance (Mishra et al., 2020) but at the cost of requiring additional information/assumptions about the average soil moisture content. EF, while much simpler to implement, has been criticised for many of its underlying assumptions including no evapotranspiration and constant hydraulic conductivity/porosity, as well as its generally poor performance at deeper layers (Albergel et al., 2008, Mishra et al., 2020).

Here, as part of the ecohydrological modelling requirement for agroforestry applications, we developed RSEEP, a model to **R**etrieve **S**oil-moisture and **E**stimate **E**cohydrological **P**artitioning. RSEEP is a simple, parsimonious conceptual ecohydrological model coupled with a retrieval algorithm that does not require information about the bulk soil moisture content, while also relaxing the assumptions of no evapotranspiration and constant hydraulic conductivity/porosity. Although RSEEP requires calibration, it only uses datasets which can

https://doi.org/10.5194/egusphere-2024-2258
Preprint. Discussion started: 31 July 2024

be easily derived from satellite products, specifically, surface soil moisture, rainfall, and potential evapotranspiration. Finally, while we demonstrate RSEEP's performance in retrieving soil moisture at different depths, performance comparison with other soil moisture retrieval methods is beyond our scope.

3.1.1 Description of RSEEP

For tractability, input (calibration) parameters are marked with ˆ to distinguish them from model coefficients and variables. There are only three parameters that require calibration: (1) $\hat{d}$, the exponent of porosity decay with depth, (2) $\hat{K}_0$, the average soil saturated hydraulic conductivity, and (3) $\hat{p}$, the exponent of soil water-potential decay with saturation (as a measure of the ease/difficulty with which water can be extracted from the soil at different saturation levels). Units of all parameters/variables are shown in square brackets throughout the paper. The schematic of the model is shown in Figure 2. Maximum canopy storage is, $S_{c_{max}}$ $[m]$, is related to Leaf Area Index, L_{AI} $[-]$, Kozak et al. (2007):

$$S_{c_{max}} = \frac{0.2 L_{AI}}{1000} \tag{1}$$

In each timestep, the Penman-Monteith potential evapotranspiration rate for grass (i.e., the reference crop), P_{ET_g} $[m/day]$, is modified to account for the additional evapotranspiration of the tree species. This modification factor, M_{ET}, is taken to be:

$$M_{ET} = 1 + \left(\frac{L_{AI} - L_{AI_g}}{L_{AI} + L_{AI_g}} \right) \tag{2}$$

where L_{AI} $[-]$ and L_{AI_g} are the Leaf Area Indices of the species under study and grass, respectively. Thus the species potential evapotranspiration will be:

$$P_{ET} = M_{ET} P_{ET_g} \tag{3}$$

Rainfall, R $[m/day]$, is added to the canopy store and if storage exceeds $S_{c_{max}}$, throughfall is generated:

$$Q_{THF} = \begin{cases} 0 & , S_c \leq S_{c_{max}} \\ S_c - S_{c_{max}} & , S_c > S_{c_{max}} \end{cases} \tag{4}$$

Actual canopy evaporation, A_{EV_c} $[m/day]$, is also subtracted from the canopy store:

$$A_{EV_c} = \begin{cases} P_{ET} & , S_c \geq P_{ET} \\ S_c & , S_c < P_{ET} \end{cases} \tag{5}$$

where S_c $[m]$ is an internal model variable which tracks the water stored in the canopy at any given time. The remaining potential evapotranspiration is then partitioned into potential evaporation for the soil compartment, P_{EV_s} $[m/day]$ and potential transpiration for the soil, P_{TR_s} $[m/day]$:

$$P_{EV_s} = (\, 1 - S_{CF} \,)(P_{ET} - A_{EV_c}) \tag{6}$$

$$P_{TR_s} = S_{CF}(P_{ET} - A_{EV_c}) \tag{7}$$

S_{CF} $[-]$ in Eq. 7 is the so-called Surface Cover Fraction (a measure of how much light the canopy structure allows to pass through or reflects back out), and is derived based on the Beer-Lambert equation (see Van Dijk & Bruijnzeel 2001):

$$S_{CF} = 1 - \exp(\, -r_E L_{AI} \,) \tag{8}$$

where r_E $[-]$ is radiation extinction coefficient which is set to 0.3 for grass and 0.7 for mature tree stands (Van Dijk & Bruijnzeel, 2001).

https://doi.org/10.5194/egusphere-2024-2258
Preprint. Discussion started: 31 July 2024

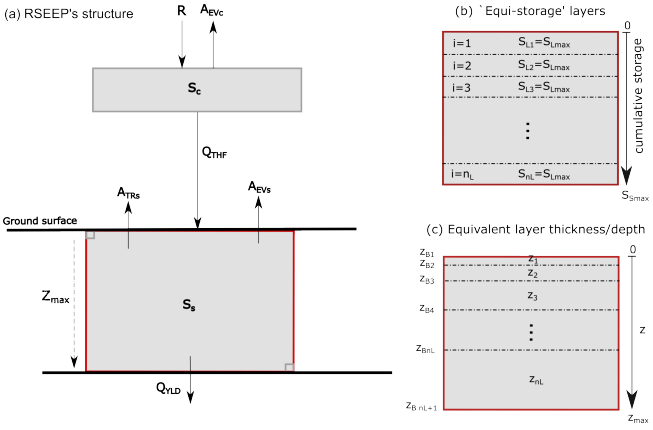

Figure 2: (a) Schematic of RSEEP's stores and fluxes. (b-c) Schematic of the layers within the soil compartment. R: rainfall; A_{EVc}: actual canopy evaporation; S_c: canopy storage; Q_{THF}; throughfall; A_{TRs}; actual transpiration; A_{EVs}: actual soil evaporation; S_s: soil water storage; Q_{YLD}: water yield; and Z_{max}: max soil depth.

In the soil compartment, from Jarvis et al. (2002), we derived the following hydraulic conductivity modifier (will be applied to Eq. 22), which relates changes in hydraulic conductivity to the changes in maximum porosity (e.g., due to changes in organic content):

$$\Delta\hat{K}_0 = 0.66\left(\frac{\phi_{max_t} - \phi_{max_{t_0}}}{\phi_{max_t} + \phi_{max_{t_0}}}\right) \tag{9}$$

where ϕ_{max_t} and $\phi_{max_{t_0}}$ are the 'current' (at time=t) and 'old' (at time=t_0) maximum porosity (i.e., at the surface). The model then requires values for soil profile depth, z_{max} $[m]$, as well as ϕ_{max} $[-]$. The former can be taken from observations or soil maps. The latter is calculated directly from the soil moisture observation at/near the surface (to which the model is calibrated) using the following equation, which accounts for the fact that porosity at the surface is likely to be higher than the value at an observation depth below the surface (note that $\hat{d}$ is always ≥ 1):

$$\phi_{max} = \phi_{obs}^{\frac{1}{\hat{d}}} + \Delta\phi_{max} \tag{10}$$

ϕ_{obs} is the porosity at the depth at which volumetric moisture content (VMC) data is available, and is taken to be equal to the maximum VMC value (i.e., during the wettest part of the record where the soil is assumed to have reached saturation). $\Delta\phi_{max}$ $[-]$ approximates the change in porosity with organic content O which is derived by differentiating a generalised porosity-soil carbon relationship (Robinson et al., 2022):

$$\Delta\phi_{max} = 0.1224\left(\frac{O_t - O_{t_0}}{O_t + O_{t_0}}\right) \tag{11}$$

The above function increases porosity as O increases, and *vice versa*. Here again, if O is unknown, or is expected to remain unchanged, O_t and O_{t_0} can be set to be equal to one another which would result in $\Delta\phi(OC) = 0$. Porosity is assumed to vary with depth using (Chen et al., 2020):

$$\phi = \frac{\phi_{max}}{\left(1 + \frac{z}{\hat{d}}\right)^{\hat{d}}} \tag{12}$$

The model keeps track of the total soil water storage, S_s $[m]$ in each time step. S_s is first divided into n_L $[-]$ number of layers with equal maximum storage values, $S_{L_{max}}$ (Figure 2b). To calculate an appropriate n_L value,

https://doi.org/10.5194/egusphere-2024-2258
Preprint. Discussion started: 31 July 2024

the thickness of the uppermost layer is set to 2 cm, for which $S_{L_{max}}$ can be calculated by integrating the porosity profile (note that the model was found to be insensitive to uppermost layer thicknesses <2 cm, hence our choice):

$$I_1(z) = \int \phi(z)dz = \phi_{max}\left(\frac{\hat{d}}{1-\hat{d}}\right)\left(\frac{\hat{d}+z}{\hat{d}}\right)^{1-\hat{d}} \tag{13}$$

$$S_{L_{max}} = \left(\frac{1}{0.02}\right) I_1(z)\Big|_0^{0.02} \tag{14}$$

Similarly the maximum storage of the soil profile is given by:

$$S_{s_{max}} = \left(\frac{1}{z_{max}}\right) I_1(z)\Big|_0^{z_{max}} \tag{15}$$

The number of layers is then given by (rounded to the nearest integer):

$$n_L = \frac{S_{s_{max}}}{S_{L_{max}}} \tag{16}$$

This way, all the layers will have the same maximum storage ($S_{L_{max}}$), which is necessary to remain mass conservative when distributing bulk soil moisture to different depths. Note that because porosity decreases with depth (see Figure 2a), the 'equi-storage' layers will have different thicknesses (Figure 2c) denoted at the boundaries of each layer by z_{B_i}, which can be back calculated by rearranging Eq.13:

$$z_{B_i} = \exp(X) - \hat{d} \quad ; \quad X = \left(\frac{1}{1-\hat{d}}\right)\ln\left(\frac{[1-\hat{d}]s_{B_i}}{\hat{d}\phi_{max}}\right) + \ln(\hat{d}) \tag{17}$$

where s_{B_i} is the cumulative sum of storage in the downward direction. Mid-point depth for each layer is calculated as the average depth within the boundaries $z_i = (z_{B_i} + z_{B_{i+1}})/2$. The increase in thickness with depth reflects the fact that soil moisture tends to become less responsive with depth, reducing the need for finer discretisation. Total soil storage, S_s, is distributed among the different layers according to a weight function:

$$w_i = \left(\frac{S_s}{S_{s_{max}}}\right)\left(\frac{S_{L_i}}{S_{L_{max}}}\right) + \left(1 - \frac{S_s}{S_{s_{max}}}\right)\left(\frac{z_i}{z_{max}}\right) \quad ; \quad i = 1, 2, ..., n_L \tag{18}$$

To ensure the weights always sum to one (to conserve mass):

$$W_i = \frac{w_i}{\sum_{i=1}^{n_L} w_i} \tag{19}$$

which leads to the following layer-wise storage:

$$S_{L_i} = W_i S_s \tag{20}$$

Thus, according to Eq. 18, in the limit that the soil is fully saturated (i.e., $\frac{S_s}{S_{s_{max}}} = 1$), all layers will be allocated equal storage (equal to their maximum storage $S_{L_{max}}$). However, as the soil becomes drier (and $\frac{S_s}{S_{s_{max}}} < 1$), deeper layers will be allocated more storage than shallow layers to reflect the fact that shallower layers tend to dry faster. This allocation preference towards the deeper layers intensifies as the soil becomes progressively drier. Also, note that the $\frac{z_i}{z_{max}}$ is a non-linear weight, the non-linearly of which increases with $\hat{d}$ $[-]$ (exponent of porosity decay with depth).

Groundwater recharge, Q_{RCH} $[m/day]$, is approximated using a Darcy-type flux, i.e., unsaturated hydraulic conductivity multiplied by a pressure head gradient (pressure head across the soil thickness):

$$Q_{RCH} = K_u\left(\frac{S_s}{z_{max}}\right) \tag{21}$$

https://doi.org/10.5194/egusphere-2024-2258
Preprint. Discussion started: 31 July 2024

where unsaturated hydraulic conductivity is assumed to deviate from the saturated conductivity according to (Iorgulescu & Musy, 1997) (note, again, that parameters with ˆ symbol are calibration parameters):

$$K_u = (\hat{K}_0 + \Delta\hat{K}_0)\left(\frac{S_s}{S_{s_{max}}}\right)^{\hat{p}} \tag{22}$$

where $\hat{p}$ $[-]$ is a decay exponent representing the decrease in soil water potential (as measure of the ease/difficulty with which water can be extracted from the soil) with saturation, and $\Delta\hat{K}_0$ is given by Eq. 9. Groundwater recharge here assumes that a water parcel needs to travel the entire thickness of the soil column before it can reach the water table and flow out of the system. Thus, at or below field capacity (e.g., in inter-storm periods) where water table tends to be lower, this assumption is more reasonable. But during intra-storm periods water tables can be at or near the surface, meaning that not only the travel distance to the water table is shorter, but also the flow occurs through the more permeable topsoil during those periods. Therefore, groundwater recharge as represented here underestimates the amount of water that leaves the system during a storm. Being 1D, our model is not capable of lateral flow routing, whether as near-surface through-flow or as overland flow. However, to account for the portion of the flow that occurs below the time resolution of our model (i.e., daily), and is absent from the Q_{RCH} term, the following procedure is implemented. In each timestep, after Q_{THF} is added to the soil, if storage exceeds maximum soil storage, fast near surface through flow, Q_{NSF} $[m/day]$ is generated which leaves the system immediately (because it flows on time-scales much shorter than daily):

$$Q_{NSF} = \begin{cases} S_s - S_{s_{max}} & , S_s > S_{s_{max}} \\ 0 & , S_s \leq S_{s_{max}} \end{cases} \tag{23}$$

Note that Q_{NSF} does not include subsurface preferential/macro-pore flow because such effects are expected to be captured in the $\hat{K}_0$ parameter during calibration, i.e., significant macro-pore flow is expected to significantly increase the bulk soil saturated hydraulic conductivity, so this effect should be included in Q_{RCH}. Total flow leaving the soil unit, or water yield, is given by:

$$Q_{YLD} = Q_{NSF} + Q_{RCH} \tag{24}$$

Total potential transpiration is distributed to different layers according to a weight function. However, this weight function differs for short-rooted plants and deeper-rooted species, to reflect the ability of deeper rooted species to adjust their water source according to water availability. The weight function is defined as:

$$x_i = \begin{cases} \left(\frac{z_{max}-z}{z_{max}}\right) & \text{, short-rooted} \\ \left(\frac{S_s}{S_{smax}}\right)\left(\frac{z_{max}-z}{z_{max}}\right) + \left(1 - \frac{S_s}{S_{smax}}\right)\left(\frac{S_{L_i}}{S_{L_{max}}}\right) & \text{, deeper-rooted} \end{cases} \tag{25}$$

According to Eq. 25, in the case of short-rooted plants, potential transpiration of top layers is higher than lower layers, irrespective of the soil wetness level. In contrast, deeper-rooted species will give higher weights to top layers if soil is closer to saturated (i.e., $\frac{S_s}{S_{smax}} \approx 1$), but will prefer wetter (lower) layers as the soil becomes drier (i.e., $\frac{S_s}{S_{smax}} < 1$). Thus, layer-wise actual transpiration is then given by (note that the weight function is normalised to ensure that the total P_{TR_s} value is conserved):

$$A_{TRs_i} = X_i\left(\frac{S_{L_i}}{S_{L_{max}}}\right)^{\hat{p}} P_{TR_s} \tag{26}$$

where

$$X_i = \left(\frac{x_i}{\sum_{i=1}^{n_L} x_i}\right) \tag{27}$$

Total actual transpiration from the soil is the sum of layer-wise transpiration values:

https://doi.org/10.5194/egusphere-2024-2258
Preprint. Discussion started: 31 July 2024

$$A_{TR_s} = \sum_{i=1}^{n_L} A_{TR_s i} \tag{28}$$

Similarly, total soil potential evaporation is also distributed amongst the layers non-uniformly, because only uppermost layers experience evaporation. To reflect this, we use an exponential function:

$$P_{EV_{s_i}}(z) = \left(\frac{2}{1+\exp(\alpha z)}\right) P_{EV_s} \tag{29}$$

which assumes potential soil evaporation equals P_{EV_s} at the surface ($z = 0$), but rapidly decreases with increasing z (depth), in such a way that it is nearly zero at around the 5 cm depth (this can be adjusted by changing α in the above equation which is set to $\alpha = 500$ in our case). Note that the above equation is a continuous function of depth and for average layer-wise potential evapotranspiration it needs to be integrated across layer boundaries:

$$I_2(z) = \int P_{EV_{s_i}}(z)dz = \left(2z - \frac{2}{\alpha}\log\left[\exp(\alpha z)+1\right]\right) P_{EV_s} \tag{30}$$

Thus, average layer-wise potential evapotranspiration will be:

$$\overline{P}_{EV_{s_i}} = \left(\frac{1}{z_{B_{i+1}} - z_{B_i}}\right) I_2(z)\Big|_{z_{B_i}}^{z_{B_{i+1}}} \tag{31}$$

Actual layer-wise soil evaporation, $A_{EV_{s}i}[m/day]$, is then calculated from layer-wise potential evaporation:

$$A_{EV_s i} = \overline{P}_{EV_{s_i}} \left(\frac{S_{L_i}}{S_{L_{max}}}\right)^{\hat{p}} \tag{32}$$

Finally, total actual soil evaporation is the sum of layer-wise actual evaporation values:

$$A_{EV_s} = \sum_{i=1}^{n_L} A_{EV_s i} \tag{33}$$

This concludes the model fluxes depicted in Figure 2 a. To summarise, RSEEP requires rainfall (R) and total potential evapotranspiration (P_{ET}) timeseries' to run. It also requires surface soil moisture timeseries for its calibration (will be discussed in 3.1.2), all of which are obtainable from satellite datasets.

3.1.2 Calibration procedure at Cruickshank Botanic Garden

First, using a sensitivity analysis, suitable ranges for individual model parameters were determined. In the absence of any prior information regarding the distribution of individual parameters we sampled 10,000 parameter-sets uniformly and randomly from their respective ranges (a 'parameter-set' = one combination of $\hat{d}$, $\hat{K}_0$ and $\hat{p}$). Note that we found our calibration procedure to be insensitive to finer sampling of the parameter space. The model was run 10,000 times, and the volumetric moisture content (VMC) at the 10 cm depth (VMC_{10}) was extracted from the model, and compared against the observed record at the same depth and for the calibration period (i.e., January-December 2021, see Fig. 4 a1/b1/c1). The observed VMC_{10} for the remaining part of the record (i.e., January-December 2022) was used for blind validation testing. At all other depths (i.e., 20, 40, 60 and 100 cm, see a2-5, b2-5, and c2-5) the entire record (i.e., January 2021-January 2023) was used for blind validation testing. Finally, based on the observed VMC timeseries at the five depths, we derived and observation-based estimate of total soil moisture (yellow solid lines in a6, b6, and c6) by calculating the weighted-average of the five observed VMCs and multiplying it by the soil thickness (which is set to be 1.2m, so that the observation-based estimate of total soil moisture does not extend far beyond the measurement depths, i.e., one meter). These weights are taken to be proportional to the layer thickness that each measurement is

https://doi.org/10.5194/egusphere-2024-2258
Preprint. Discussion started: 31 July 2024

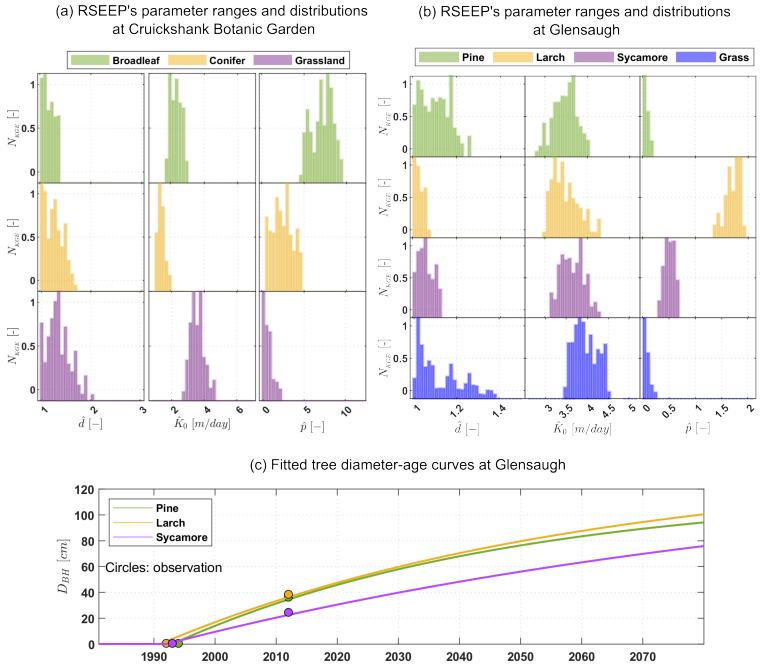

Figure 3: Ranges and distributions of model parameters (a) at Cruickshank Botanic Garden, and (b) at Glensaugh; N_{KGE}= normalised KGE. (c) Tree diameter-age curves at Glensaugh.

assumed to represent, which are, 0-15 cm, 15-30 cm, 30-50 cm, 50-80 cm, and 80-120 cm, for VCM_{10}, VCM_{20}, VCM_{40}, VCM_{60}, and VCM_{100}, respectively.

For performance metric, we used the Kling-Gupta Efficiency (KGE) because it includes correlation, variability bias as well as mean bias:

$$KGE = 1 - \sqrt{(r-1)^2 + \left(\frac{\sigma_{sim}}{\sigma_{obs}} - 1\right)^2 + \left(\frac{\mu_{sim}}{\mu_{obs}} - 1\right)^2} \tag{34}$$

where r is the linear correlation coefficient between the simulated ($_{sim}$) and observed ($_{obs}$) records, σ is standard deviation, and μ is mean. Rather than the best model, the top 1% of the models in terms of their KGE values during the calibration period (i.e., at the 10cm depth and for the January-December 2021, see a1, b1 and c1) were retained as 'acceptable', to provide some measure of parameter variability. Although, many other potential sources of uncertainty remain which are difficult to quantify in ecohydrological modelling in general, and in predicting soil moisture in particular. We discuss the sources of uncertainty in section 6.

3.2 Coupling RSEEP to a soil carbon model

3.2.1 Rothamsted carbon model

The Rothamsted carbon model (RothC, Coleman & Jenkinson 2014) distinguishes five soil organic matter pools; decomposable and resistant plant material (DPM $[tC/ha]$ and RPM $[tC/ha]$), humified soil organic material (HUM $[tC/ha]$), soil microbial biomass (BIO $[tC/ha]$) and an inert organic matter pool (IOM $[tC/ha]$). Plant inputs to the soil partition into DPM and RPM according to a DPM/RPM ratio (R_{DR}) which is assumed to be

https://doi.org/10.5194/egusphere-2024-2258
Preprint. Discussion started: 31 July 2024

0.25 for tree sites, and 0.67 for grass/pasture sites (Ražauskaitė et al., 2020). Each active organic matter pool (Y) decomposes according to a first order exponential equation of the form:

$$dY = Y \times (1 - \exp(-k.a.b.c.t)) \tag{35}$$

where $k\ [1/yr]$ is the decomposition rate constant for pool Y (equal to 10, 0.3, 0.66 and 0.02 for DPM, RPM, BIO and HUM, respectively), $a\ [-]$ is a temperature rate modifier, $b\ [-]$ is a soil moisture rate modifier, $c\ [-]$ is soil cover rate modifier, and t is time-scale which is set to $\frac{1}{365}$ (i.e., daily) in our study. In each timstep, the decomposed material of each pool (dY) is then distributed among the CO_2, HUM and BIO pools according to pre-determined fractions (see Coleman & Jenkinson 2014 for details). Thus, the only unknowns in RothC are the initial (equilibrium) values for each pool (i.e., at $t = 0$) as well as the annual plant inputs at equilibrium ($I_{A_0}\ [tC/ha]$). To calculate these, it is commonly assumed that prior to any interventions (tree planting in our case) the soil has been in a state of equilibrium where its organic carbon content remains constant with time (in our case this would be 52 tC/ha, see table 1). By running RothC for 10,000 years using fixed climate data (i.e., the 2015-2022 data is looped), and through a minimisation process, the initial values for each pool as well as the I_{A_0} that would result in 52 tC/ha of soil organic content at time $t = 0$ can be found (see Coleman & Jenkinson 2014 for more details). Equilibrium daily plant inputs (I_{D_0}) are then calculated from the annual plant inputs:

$$I_{D_0} = f_{LAI} I_{A_0} \tag{36}$$

where

$$f_{LAI} = \frac{R_{LAI}}{\max(R_{LAI})} \tag{37}$$

and

$$R_{LAI} = \begin{cases} 0 & ; \ -\frac{\partial}{\partial t} L_{AI}(t) < 0 \\ -\frac{\partial}{\partial t} L_{AI}(t) & ; \ -\frac{\partial}{\partial t} L_{AI}(t) \geq 0 \end{cases} \tag{38}$$

This equation assumes that maximum plant inputs occur at the same time as maximum rate of reduction in L_{AI} occurs. In addition, when L_{AI} increases with time or remains constant, plant inputs to the soil are assumed to be zero according to this equation. Finally, RothC also requires soil cover (which is set to zero for bare soil and 1 otherwise) as an input to determine the value of c in Eq. 35. We set soil cover to 1 when $L_{AI} > \min(L_{AI})$ and 0 otherwise.

At a given time, the total soil organic carbon ($TOC\ [tC/ha]$) is the sum of the values in the five pools. Percentage soil organic matter can then be calculated from:

$$O\ [\%] = \frac{1000 \times TOC}{A z_{max} B_D} \times 100 \tag{39}$$

where $A\ [m^2]$ is land area, $z_{max}\ [m]$ is soil thickness, and $B_D\ [kg/m^3]$ is soil bulk density. Thus, when linking RSEEP with RothC, changes in organic content with time will be fed into Eqs. 9 and 11 to account for changes in soil water retentiveness due to organic content change. On the other hand, note that RothC in its original from applies a simple soil moisture accounting procedure in which total soil moisture deficit is assumed to be given by:

$$D_{SM} = R - P_{ET} \tag{40}$$

where $R[m]$ is rainfall, and $P_{ET}[m/day]$ is the Penman-Monteith potential evapotranpiration rate. $SMD\ [m]$ is capped at:

$$D_{SM_{max}} = 0.0043(20 + 1.3P_{clay} + 0.01P_{clay}^2)z_{max} \tag{41}$$

https://doi.org/10.5194/egusphere-2024-2258
Preprint. Discussion started: 31 July 2024

where P_{clay} [%] is clay content. Field capacity is assumed to be $D_{field} = 0.444 \times D_{SM_{max}}$. However, when linking RothC with RSEEP this entire procedure is overwritten, and D_{SM} is calculated directly from RSEEP's output, namely: $D_{SM} = S_{s_{max}} - S_s$ (see section 3.1.1).

Finally, note that RothC's original soil moisture rate modifier (b) remains equal to its maximum value (i.e., 1) when $D_{SM} < D_{field}$ and decreases toward its minimum (i.e., 0.2) as D_{SM} increases above D_{field}. Therefore, in its original form, RothC ignores reductions in decomposition rate under waterlogged conditions (i.e., when oxygen is limited), and instead it only considers reductions in decomposition rate under dry conditions (i.e., when water is limited). For this reason, in this study we used a slightly different soil moisture rate modifier (Smith et al., 2010) that also decreases (from 1 toward 0.2) as soil oxygen levels decrease.

3.2.2 Representing vegetation growth

It is common to assume that tree-growth broadly follows an exponential function (Schelhaas et al., 2018). We assumed the following relationship between diameter at breast height, D_{BH} [cm], and tree age t [yr]:

$$D_{BH}(t) = D_{BH_{max}} \left(1 - \exp\left(-\hat{\beta}[t - \hat{t}_0] \right) \right) \tag{42}$$

where β [$-$] and t_0 [yr] are parameters controlling the shape of the curve (to be determined via calibration), and $D_{BH_{max}}$ [cm] is the maximum DBH for a given species; upper bound values for $D_{BH_{max}}$ (for ages>150 years) is taken to be 140 cm for Hybrid Larch (Larsson-Stern, 2012), 120 cm for Scots Pine (Hall & Bunce, 2011) and 145 cm for Sycamore (Hall & Bunce, 2011). Further, for the tree species at Glensaugh, there exists allometric equations of the form (assumes 45% organic content for biomass):

$$\ln(B_A) = 0.45 \left(\frac{P_D}{1000} \right) (\eta + \lambda \times ln(D_{BH})) \tag{43}$$

to estimate above-ground biomass ($B_A[tC/ha]$) from D_{BH}, where P_D [$-$] is the plantation density (=400 stems/ha at Glensaugh) and η [$-$] and λ [$-$] are species-specific coefficients. η = -2.26, -2.029 and -2.455, for Hybrid Larch (Nan et al., 2012), Scots Pine (Lim & Cousens, 1986) and Sycamore (Bunce, 1968), respectively; and λ = 2.298, 2.289, and 2.354, respectively. Following Cairns et al. (1997), we also estimate below-ground biomass (B_B [tC/ha]) from above-ground biomass (B_A) using (also assumes 45% organic content for biomass):

$$B_B = 0.45 \left(\frac{P_D}{1000} \right) \exp\left(-1.0587 + \ln\left(1963.6 \frac{B_A}{P_D} + 0.2840 \right) \right) \tag{44}$$

The Leaf Area Index (L_{AI}) data, which is used by the ecohydrological model (see Eqs. 2, 8 and 1) is not available at the site. We thus use species-specific maximum L_{AI} values obtained from the available literature: 5.7 for Hybrid Larch (Gower et al., 1990), 2.73 for Scots Pine (Bealde et al., 1982), and 5.6 for Sycamore (Elsherif al., 2023), all between 70-90 years old, and 2 for Rye grass (Simon & Lemaire, 1987). We increased the tree L_{AI} values by another 10% to account for the fact that they are not fully mature (i.e., not 150-200 years old). Similar to the botanic garden site (section 2.1), for the evergreen species (i.e., Pine) we assume a time invariable L_{AI}, while for the two deciduous species (i.e., Larch and Sycamore) and grass a trapezoidal shape was employed with the minimum value set to 1.5 for trees and 1 for grass. The timing of rises, peaks and decreases of this trapezoid were also taken to be the same as those at the botanic garden site. Note that the maximum L_{AI} values above assume mature species, meaning that they will be significant overestimation of L_{AI} at the early stages of the agroforestry experiment (except for grass which had existed pre-agroforestry). To account for this, species L_{AI} vary with time according to an age fraction, f_{age}:

$$L_{AI}(t) = f_{age}(t) L_{AI_\infty} + (1 - f_{age}(t)) L_{AI_g} \tag{45}$$

where L_{AI_∞} is the leaf area index time series of mature species, L_{AI_g} is that of grass (for grass they are equal to one another), and:

$$f_{age}(t) = \begin{cases} 1 & ; \text{ for grass} \\ \frac{D_{BH}(t)}{D_{BH_{max}}} & ; \text{ for trees} \end{cases} \tag{46}$$

https://doi.org/10.5194/egusphere-2024-2258
Preprint. Discussion started: 31 July 2024

Eq. 45 varies tree L_{AI} on a sliding scale between grass and fully grown trees depending on age. The same logic also applies to the $r_E[-]$ parameter (radiation extinction coefficient, see section 3.1.1):

$$rE(t) = f_{age}(t) r_{E_\infty} + (1 - f_{age}(t)) r_{E_g} \tag{47}$$

where $r_{E_\infty} = 0.7$ for trees (but $=r_{E_g}$ for grass), and $r_{E_g} = 0.3$. Similarly, the DPM/RPM ratio (R_{DR}, see section 3.1.1) varies with age according to:

$$R_{DR}(t) = f_{age}(t) R_{DR_\infty} + (1 - f_{age}(t)) \times R_{DR_g} \tag{48}$$

where $R_{DR_\infty} = 0.25$ for trees (but $=R_{DR_g} = 0.67$ for grass), and $R_{DR_g} = 0.67$. Finally, non-equilibrium annual plant input to the soil at time t ($I_A(t)$ $[tC/ha]$), is needed to run the carbon model in 'forward' (future) mode (see section 3.2.1). At any given time, plant input is calculated using:

$$I_A(t) = \begin{cases} I_{A_0} & ; \quad t < 1988 \\ I_{A_0} + f_{age}(t) \hat{I}_{A_\infty} & ; \quad t \geq 1988 \end{cases} \tag{49}$$

where I_{A_0} $[tC/yr]$ is the equilibrium input (at t=0) calculated by running RothC in 'equilibrium' mode (see section 3.2.1), and $\hat{I}_{A_\infty}$ $[tC/ha]$ is a future equilibrium input (at $t \sim \infty$, to be determined via calibration) representing a future state in which trees have reached maturation, i.e., their D_{BH} has plateaued due to the exponential diameter-age curve in Eq. 42. In our case, this would occur c.a. after 200 years depending on the species (see Figure 3 c). For grass however, $\hat{I}_{A_\infty}$ would represent the additional organic carbon inputs due to introduction of grazing post-agroforestry in 1988, rather than vegetation growth/maturation. Thus, Eq. 49 will yield I_{A_0} for the pre-agroforestry period, but increases plant input in the post-agroforestry period. Note that daily plant inputs are calculated from the annual values using Eq. 36.

3.2.3 Calibration procedure at Glensaugh

We apply the same calibration procedure that was used at the botanic garden site (section 3.1.2) to determine the values for the three calibrated RSEEP parameters (i.e., $\hat{d}$, $\hat{K}_0$ and $\hat{p}$). For forcing and check data, we use the 2022 dataset presented in Figure 1 d, and we set the tree ages (for L_{AL} calculation in Eqs. 45 and 42) to 34 years (=2022-1988). This approach results in 100 (i.e., top 1% of 10,000) RSEEP parameter-sets per species. Parameter ranges and distributions at Glensaugh are shown in Figure 3 b. KGE performance in the top 1% of the models ranged between 0.68-0.83 for Pine, 0.7-0.74 for Larch, 0.68-0.74 for Sycamore, and 0.43-0.61 for Grass.

Also recall from section 3.2.2 that there are three additional unknown parameters: $\hat{\beta}$, $\hat{t}_0$ and $\hat{I}_{A_\infty}$. To determine these parameters, we use a minimisation procedure that utilises the data in Table 1. For the RSEEP parameter-set that produces the closest predictions to the median of all RSEEP predictions, the minimisation process iteratively selects different values for these three parameters, runs the coupled model, and refines them, until: (i) the predicted soil carbon stocks matches the 2012 value in Table 1 as closely as possible (which would constrain $\hat{I}_{A_\infty}$); (ii) $\hat{t}_0$ captures the onset of tree heights reaching 1.3m (third column in Table 1) as closely as possible; (iii) and D_{BH} (Eq. 42) matches the values in the last column as closely as possible (which would constrain $\hat{\beta}$). Figure 3 c shows the resulting D_{BH} curves for each tree species. Parameter values as well as past and future equilibrium inputs for the different species are listed in Table 2.

3.2.4 Calculating the relative impacts of agroforestry at Glensaugh

To disentangle the impact that trees have within the silvopastoral system, we first calculate the net change in the pasture (control) site across time by subtracting our model prediction for the quantity $\pi_p(t)$ ('p' for pasture) at any time $t \geq 1988$, from its predicted value π_{p_0} at time $t = 1987$, to give $\Delta\pi_p(t) = \pi_p(t) - \pi_{p_0}$ as a function of time. Here we consider the following quantities as π: soil carbon stocks, and total carbon stocks (soil + biomass carbon), canopy evaporation, soil evaporation, transpiration, soil water storage deficit, water yield (total outflow). We then repeat the same process for the silvopasture sites to obtain $\Delta\pi_s(t) = \pi_s(t) - \pi_{s_0}$. We then

https://doi.org/10.5194/egusphere-2024-2258
Preprint. Discussion started: 31 July 2024

Table 2: Fitted tree-growth parameters at Glensaugh. I_{A_0}: range of equilibrium annual plant input to the soil at $t = 0$, i.e., before trees were planted. $\hat{I}_{A_\infty}$: equilibrium annual plant input at a future time, $t \to \infty$, when trees have reached maturation. $\hat{\beta}$ and $\hat{t}_0$ are coefficients of tree growth curve in Eq. 42.

Species	I_{A_0} $[tC/ha]$	$\hat{I}_{A_\infty}$ $[tC/ha]$	$\hat{\beta}$ $[-]$	$\hat{t}_0$ $[yr]$
Grass	2.11:2.37	1.22	-	-
Sycamore	2.33:2.66	32.98	0.0085	5
Pine	2.37:2.65	16.95	0.018	6
Larch	2.37:2.64	24.6	0.0144	4

calculated a percentage change relative to the conditions in 1987 using: $\%\text{change} = \frac{\Delta\pi_s(t) - \Delta\pi_p(t)}{\pi_{p_0}} \times 100$. Finally, for each scenario there are 400 model predictions (100 RSEEP parameter-sets $\times$ 4 future climate models). When calculating the relative impacts, we thus consider all possible differences, i.e., 400 $\times$ 400=160,000 between each silvopasture scenario at time t and the pasture case. The median of these 160,000 values are presented in Figure 6, 20, 40 and 80 years after planting. The full range of model predictions are also shown in Tables A1, A2 and A3 in the Appendix.

4 Results

4.1 RSEEP's soil moisture retrieval performance

Figure 3 a shows the parameter distributions for each species at Cruickshank Botanic Garden, where x-axes are parameter ranges and y-axes are normalised KGE values. All parameters seem to have a well defined distribution indicating that the model has been sensitive to them. In interpreting the KGE values, note that KGE can range from $-\infty$ (i.e., the worst possible fit) to 1 (i.e., perfect match between observation and prediction), however not all negative KGE values are necessarily indicative of 'bad' performance. When using mean flow (or soil moisture in our case) as benchmark Knoben et al. (2019) showed that models with KGE>-0.41 improve on the mean flow benchmark. Thus, here we also take KGE>-0.41 to be the threshold for acceptable performance, at least during the blind validation test. Also note that in Figure 4, the only information available to the model during calibration is constrained to within the first half of the record and to the 10 cm depth (marked by dashed red lines in panels a1, b1, and c1). The model is 'blind' to the second half of the record in a1, b1, and c1, as well as to the entire record in all other panels. Finally, in all panels, median KGE values of the top 1% models are reported with their minimum and maximum shown in brackets.

Under the broadleaf tree, the model is able to provide very good fits to the observed soil moisture timeseries during the calibration period, indicated by the median (and min:max) KGE value of 0.81. Curve-fitting performance slightly worsens during the second half of the record (i.e., blind validation) at the 10 cm depth (panel a1), where median KGE is 0.67, though still considered good fit. The model maintains a similar goodness-of-fit level during the blind validation test at the 20cm depth (panel a2, KGE=0.68), but further deteriorates at the 40cm depth (panel a3, median KGE=0.42). This trend continues at the 60cm and 100cm depths where median KGE values are 0.06 and -0.05, respectively. Although relative to the mean of record as benchmark (which would yield a KGE value of -0.41) these values are all considered improvements in predictive power, particularly because they broadly capture the soil moisture dynamics. Similar trends can be observed under the conifer tree (b1-b6). In the grassland case, the model performs well at all depths (with a median KGE=0.75 at 10cm depth and KGE=0.59 at 100cm depth).

4.2 Sensitivity of RothC to soil moisture accounting method

To test the impact of a different soil moisture representation on RothC's carbon storage estimates, we compare RothC's predictions when coupled with RSEEP versus when it is not. RothC without coupling uses rainfall minus potential evapotranspiration (or 'effective rainfall') to update its soil moisture in each time step, whereas

https://doi.org/10.5194/egusphere-2024-2258
Preprint. Discussion started: 31 July 2024

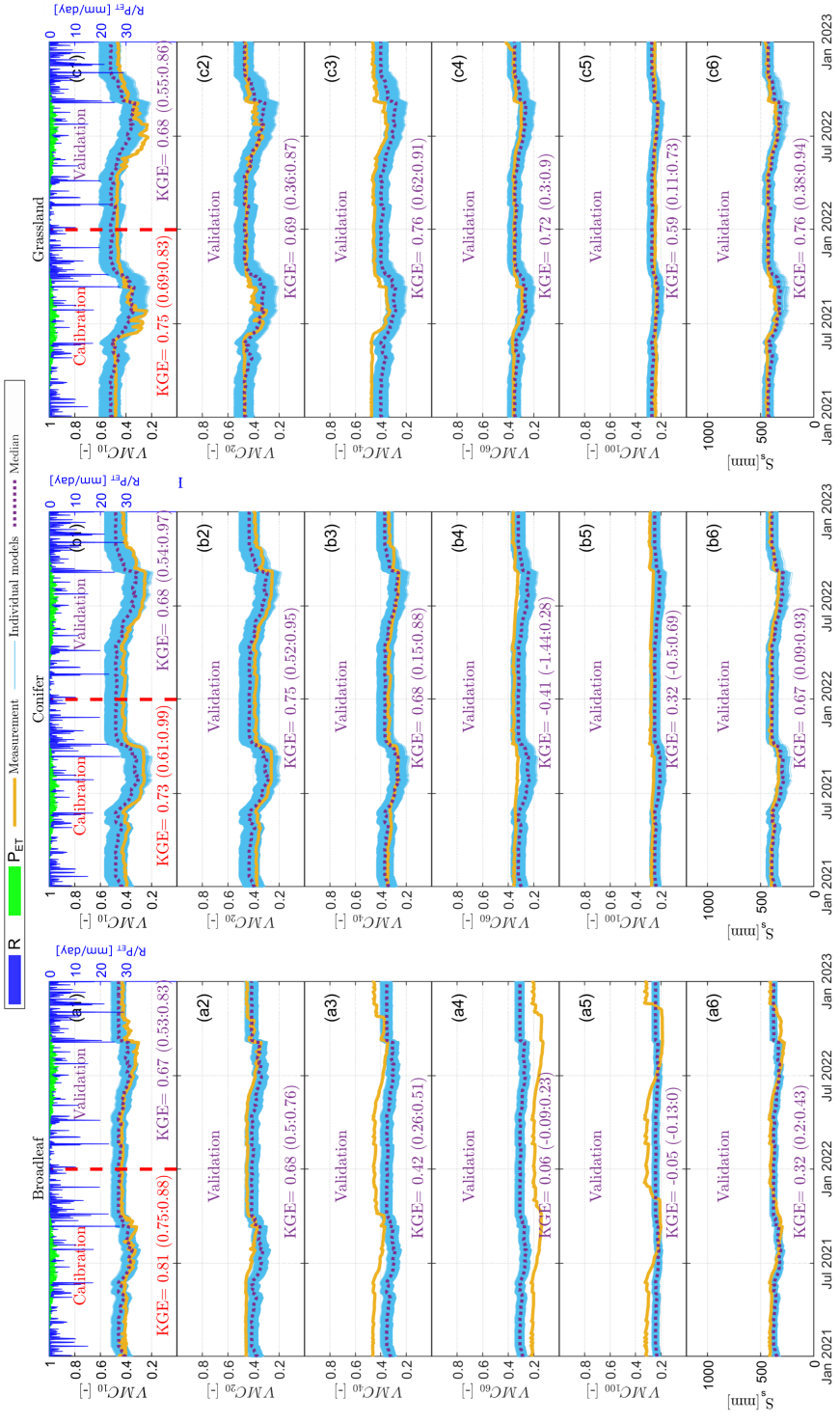

Figure 4: (a1-a5): predicted versus observed volumetric moisture content (VMC) timeseries at different depths and under the broadleaf tree at the botanic garden site. (a6): total soil moisture at the top 1 meter of the soil. (b1-b6) show the same results but under the conifer tree; (c1-c6) are for the grassland site. In each panel solid yellow lines are observed values and shaded blue bands are ensembles of model predictions.

https://doi.org/10.5194/egusphere-2024-2258
Preprint. Discussion started: 31 July 2024

when coupled to RSEEP, that procedure is replaced by outputs directly from RSEEP. Figure 5 a1 shows the annual average S_s values resulting from the two models. Dashed lines represent the water storage capacities in each case. There is a stark difference in the magnitude of annual average storage between RothC and RothC+RSEEP. However, RothC is not necessarily affected by the absolute magnitude of storage, rather by its value relative to the maximum (see soil-moisture rate modifying factor in section 3.2.1). For this reason we also show the normalised $\overline{S}_s$ values in panel a2, where $\overline{S}_s$ values in panel b1 are divided by their respective maximum (dashed lines in panel b1).

From a2, it can be seen that RothC+RSEEP predicts a drier soil when compared to RothC. From b3, drier soils under RothC+RSEEP lead to 28% lower soil carbon stock under Larch (by the end of the record in 2080 and using the dotted lines); the same value is a 20.1, 9.2 and 5.6% lower carbon stock under Sycamore, Pine and Grass, respectively. Given that the median change in annual 'effective rainfall' ($R-P_{ET}$) between 1980-2080 has been -190mm (i.e., a reduction), our results suggest that improving RothC's soil moisture representation could reduce its carbon storage predictions by 0.15, 0.11, 0.05, and 0.03% per mm reduction in effective rainfall under Larch, Sycamore, Pine and Grass, respectively, or an average of 0.08%/mm across all sites.

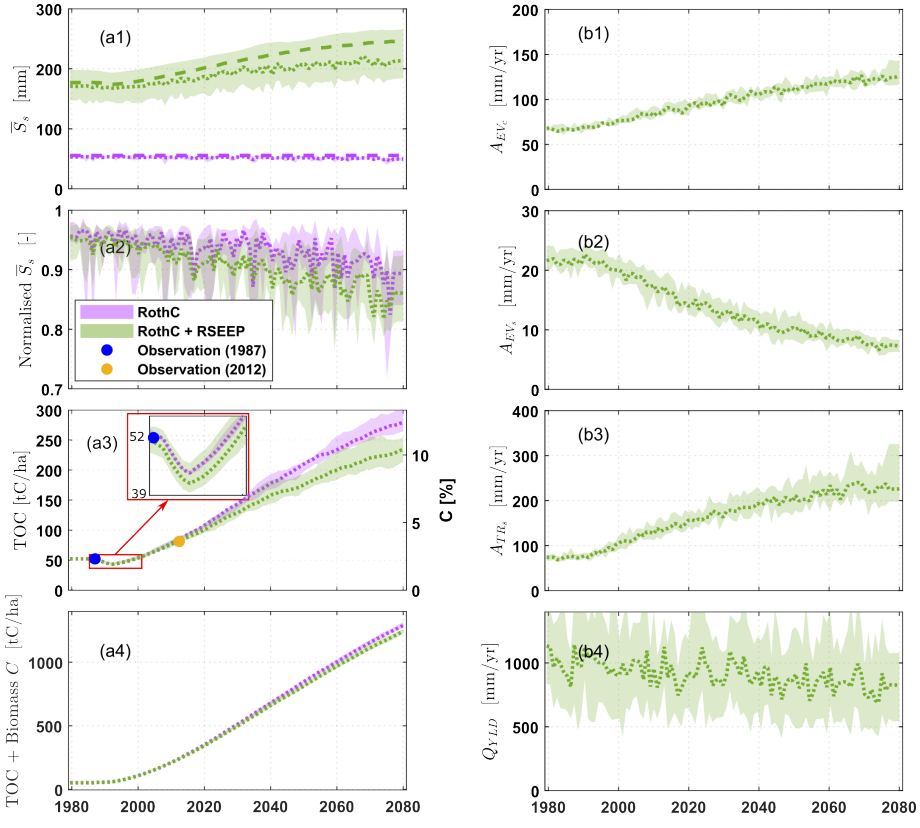

Figure 5: a1-a4: sensitivity of RothC to soil moisture treatment method at the Larch site. b1-b4: the associate (eco)hydrological fluxes from the coupled RSEEP+RothC model; A_{EV_c} = annual canopy evaporation, A_{EV_s} = annual soil evaporation, A_{TR_s} = annual transpiration, Q_{YLD} = annual water yield. Shaded bands represent modelling + climate data variability. Dotted lines are the median of all 400 model predictions (i.e., all combinations of the 100 RSEEP parameter-sets & the 4 versions of the future climate dataset). Dashed lines in a1 are maximum soil water storage capacity.

https://doi.org/10.5194/egusphere-2024-2258
Preprint. Discussion started: 31 July 2024

4.3 The relative environmental impacts at Glensaugh

From Figure 6 a, under the current emission scenario (RCP6.0), total annual rainfall increases then decreases across the three time-slices, whereas potential evapotranspiration increases monotonically. Relative to the conditions before converting pasture to silvopasture, the 20th and 40th years are wetter because in those years rainfall increases more than evapotranspiration, whereas the 80th year is the driest of the set.

From b1, soil carbon stocks generally increase with time under all scenarios. 20 yrs after conversion to Pine/Sycamore (but not Larch) silvopasture, soil carbon is reduced. This mimics the disturbance to the soil when trees are planted (see e.g., the zoomed panel in Figure 5 a3; which happens in our model by setting I_{A_0} to zero from the onset of tree plantation until $t = \hat{t}_0$). When considering the total carbon stocks (in b2), which includes the above- and below-ground biomass estimates, all scenarios boost carbon storage relative to the pasture base-case, with Larch having the largest impact in all years, closely followed by Pine. Sycamore's contribution to total carbon stocks after 20 years is relatively small (i.e., 13% compared to 87% and 65% for Larch and Pine, respectively), but it increases considerably 40 and 80 years after conversion; though remains around half the contributions of Larch and Pine. From b3, annual average soil water storage deficit increases with time as trees grow indicating drier soil. The amount by which conversion to silvopasture makes the soil drier is similar for all species until the 40-year mark, but at the 80-year, Pine leads to a significantly drier soil followed by Sycamore. Given that the 80th year is the driest year examined here, it is notable that the soil under Larch exhibits the smallest increase in storage deficit.

From c1, canopy evaporation increases monotonically with time and in the order of Pine>Larch>Sycamore. From c2, soil evaporation decreases monotonically with time, despite the monotonically increasing atmospheric demand (a), which is related in our model to canopy closure. From c3, conversion to silvopasture dramatically increases transpiration and in the order of Pine>Larch>Sycamore. From d1, in terms of the total outflow from the soil unit, or water yield, conversion to silvopasture decreases annual water yield substantially and in the order of Pine>Larch>sycamore up until the 40-year mark, then in the order of Pine>Sycamore>Larch at the 80th year.

5 Discussion

5.1 Strengths and weaknesses of RSEEP

If soils can be assumed to have reached saturation during the wettest part of the record (which is a reasonable assumption at Cruickshank Botanic Garden), we can take the maximum observed soil moisture content at each depth to be equal to porosity at that depth. In that case, from Figure 4, the soil column under the broadleaf tree would have the following porosity profile: 0.43, 0.45, 0.46, 0.21 and 0.32, at 10cm, 20cm, 40cm, 60cm, and 100cm depths, respectively. Such a profile could indicates changes in soil composition with depths, which would explain the clearly different soil moisture dynamics at the different depths through, e.g., changes due to hydraulic conductivity (Gardner, 1983). It is also possible that the irregularity is due to presence of macropores caused by tree tap-roots (Demand et al., 2019) and/or earthworms (Rutgers et al., 2016). Whatever the cause, the underlying physical processes responsible for such behaviour are absent from our simple model. RSEEP assumes that both soil porosity and hydraulic conductivity monotonically decrease with depth, and is thus not equipped to capture deviations from these assumptions.

Similar analysis applies to the conifer site while at the grassland site the model performs well at all depths (with a median KGE=0.75 at 10cm depth and KGE=0.59 at 100cm depth). This is not surprising because the maximum observed VMC values are: 0.48, 0.47, 0.46, 0.36, 0.24, at depths=10cm, 20cm, 40cm, 60cm and 100cm, respectively, indicating that porosity and hydraulic conductivity here are more likely to be monotonically decreasing functions of depth, just as it is assumed by RSEEP. While it is not particularly difficult to relax these assumptions in the model, the downside is additional calibration/uncertain parameters which would in turn require additional datasets to constrain. We have developed RSEEP with large-scale applicability in mind. At those scales, detailed below-ground information is simply not available for calibration of any additional model parameters. It is worth noting that despite the simple model structure, total soil storage behaviour (panel a6)

https://doi.org/10.5194/egusphere-2024-2258
Preprint. Discussion started: 31 July 2024

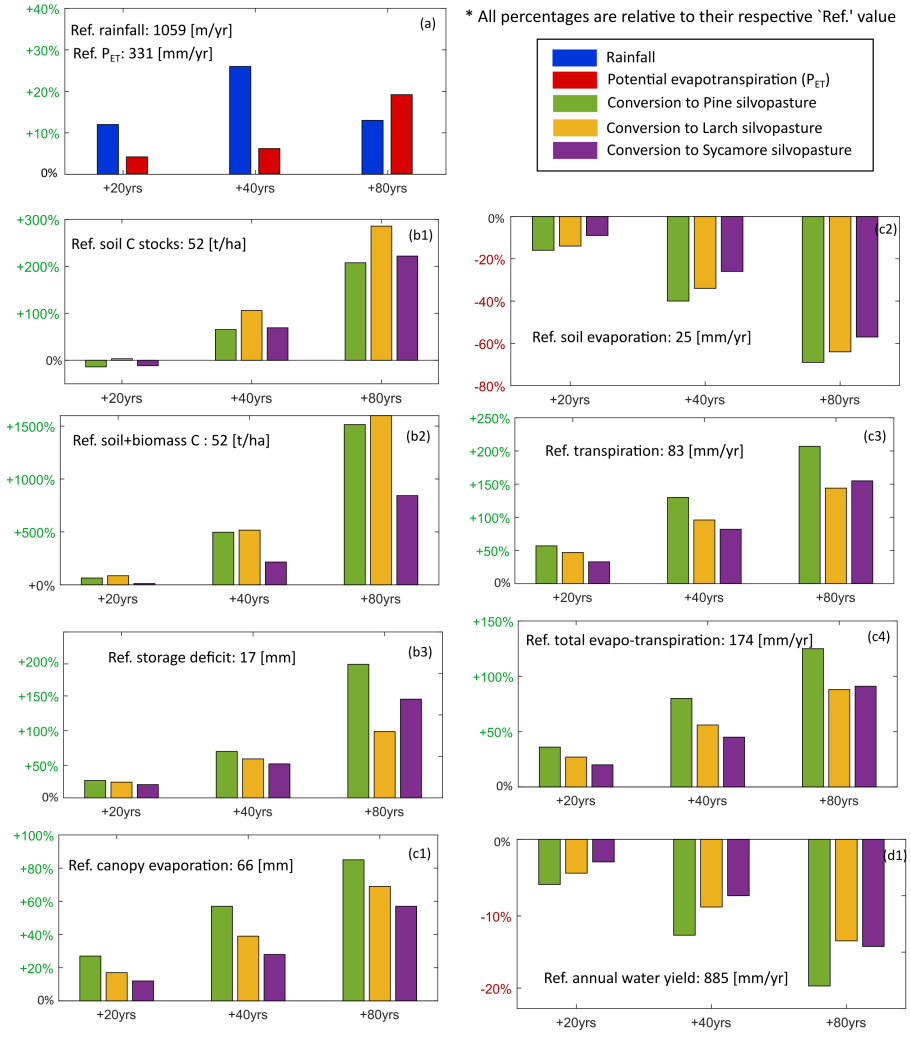

Figure 6: The environmental impacts of converting pasture to silvopasture at Glensaugh after 20, 40 and 80 years (calculated annually). Bars show median (of 160,000) model predictions. All percentages are relative to their respective reference value ('Ref.') which represents the pasture base-case at time $t = 0$, i.e., in 1987. The full range of annual values are shown in Table A1. The full range of values during the summer and winter seasons are shown in Tables A2 and A3, respectively.

https://doi.org/10.5194/egusphere-2024-2258
Preprint. Discussion started: 31 July 2024

is captured well, with median KGE well above the -0.41 threshold. This is noteworthy because in soil carbon turnover models such as RothC, it is often the total soil moisture (deficit) that is needed run the model.

Thus, these results suggest that (i) RSEEP can capture the dynamics of bulk soil moisture (rather than that at specific depths) fairly well, even if the assumptions underlying the model do not strictly hold everywhere along the soil profile; (ii) RSEEP can estimate soil moisture at specific depths fairly well in soils in which the model assumptions are more likely to hold. Application of our model to different soil types/thicknesses and more sites would provide more confidence that these conclusions generally hold.

5.2 Impact of soil moisture accounting procedure on RothC

In section 4.2 we found that including the various ecohydrological water fluxes (i.e., RothC+RSEEP) in soil water balance estimation resulted in a lower soil carbon storage than estimates using RothC alone. Accordingly, performing a more elaborate soil moisture accounting, compared to RothC's default setting, on average can lead to a 0.08% lower soil carbon estimation per mm reduction in 'effective rainfall' (i.e., rainfall - potential evapotranspiration). While the impact of different soil-moisture decomposition rate modifying functions on RothC's performance has been extensively studied (e.g., Falloon et al. 2011, Bauer et al. 2008 and references therein), to our knowledge the impact of different soil moisture accounting procedures on RothC's performance is untested. Thus, our results provide a first insight into the possible sensitivity of RothC-based soil carbon estimates to the choice of soil moisture accounting method. Our results suggest that more elaborate accounting procedures (than RothC's default) should be used where possible. They also indicate that a coupled water-carbon approach to soil carbon cycling could be important, particularly over longer time-scales and when considerable future changes to soil moisture regimes are likely. Testing RothC in conjunction with different soil moisture treatments as well as at different sites would strengthen these findings.

5.3 Water-carbon dynamics of the silvopastoral experiment at Glensaugh

5.3.1 Carbon storage potential

Our pasture to silvopasture conversion scenarios initially reduce soil carbon stocks (figure 6b1) due to disturbance of the soil at the onset of conversion, in line with observations globally (Guo &Gifford, 2002), and in the UK (Upson et al., 2016). Our results suggest that 20 years after planting, soil carbon stocks are yet to recover to their pre-conversion levels under Pine and Sycamore, but if Larch is planted recovery could be faster. For t>=40 years, all scenarios increase soil carbon substantially with Larch having the largest impact. Pine and Sycamore have similar impacts with Sycamore outperforming slightly. At the 40-year mark, we estimate that these scenarios will have increased soil carbon by 66-107% relative to pasture, yielding an annual rate of change of +0.85 to +1.4 t/ha/yr which is within the rather wide -10.6 to +5.1 t/ha/yr range reported for 30-40 year-old afforestation cases across Scotland, and within the narrower -2 to +3.1 t/ha/yr range reported for afforestation on podzolic soils (Lilly et al., 2016). It is also within the 0.55 to 2 t/ha/yr range estimated for silvopasture globally (Lal, 2018).

When also considering biomass carbon, all scenarios positively impact carbon storage (even at the 20-year mark), with Larch having the largest impact closely followed by Pine, while Sycamore underperforms by at least 50% in all the years examined here. This seems to be related to the growth-rates of these species observed at Glensaugh which are in the order of Larch>Pine>Sycamore (see Figure 3 c). It is notable that despite the significantly slower growth, Sycamore's contribution to soil carbon is slightly higher than that of Pine. Through a meta-analysis, Vesterdal et al. (2012) report a higher carbon mineralisation under Sycamore than under conifers, and even most other broadleaves (except for Ash), with litterfall quality (foliar N, Ca and Mg, and to some extent lignin concentrations) correlating best with carbon turnover, but they did not examine the possible effects of root litter inputs. Deciduous species are shown to have greater fine root biomass than evergreen species (Finér et al., 2007) which could also be a contributing factor in Sycamore's slightly higher soil carbon turnover (despite its significantly slower growth). While our model is not capable of capturing either of these effects explicitly, it can capture them implicitly into its equilibrium plant input estimates. Equilibrium

https://doi.org/10.5194/egusphere-2024-2258
Preprint. Discussion started: 31 July 2024

inputs estimated by our model are in the order of Sycamore>Larch>Pine (see Table 2) which seems consistent with the higher litterfall quality and/or fine root biomass of deciduous trees.

Observations at Glensaugh show that 24 years after conversion to silvopasture, the Pine site maintained a healthy-looking pasture whereas herbaceous vegetation had visibly suffered under the Larch and Sycamore plots due to canopy closure (Beckert et al., 2015). This may suggest that under the current management and plantation density at Glensaugh, silvopasture is likely to work well for a finite period of time, which could be extended if evergreen species are planted. This could impact management decisions on rotation length. Our soil carbon estimates provide insight at different points in time assuming that the management decision will be to maintain tree cover up to that point in time. Our results provide little insight regarding the aftermath of a fixed rotation management scenario in which trees are felled. Such scenarios should be investigated separately.

Since the average rotation-length in Scotland is around 40 years (Lilly et al., 2016), we expect our predictions at the 40-year mark to be more meaningful in the context of Scottish agroforestry. We conclude that at Glensaugh and under the current emission scenario (RCP6.0) (i) a conifer silvopasture scenario is likely to outperform a broadleaf scenario in terms of biomass carbon storage due to the significantly higher growth-rates of conifer species at this site; (ii) a deciduous silvopasture scenario at this site is likely to outperform an evergreen scenario in terms of soil carbon turnover due to higher litterfall quality and/or greater fine root carbon inputs. The two together seem consistent with the fact the deciduous conifer scenario has largest overall impact in terms of carbon storage at Glensaugh.

5.3.2 Impacts on soil water availability

Converting pasture to silvopasture at Glensaugh generally increases soil water storage deficit (figure 6b3), meaning that trees tend to make the soil drier over time and as they grow. This is expected given the significant increase in transpiration rates seen in panel c3. The direct correlation between transpiration (in c3) and storage deficit (in b3) is an indication that the drier soils are primarily a result of higher transpiration of trees, in line with experimental (e.g., Soulsby et al. 2017b) and modelling (e.g., Stevenson et al. 2023) studies in the region. This could have implications for water availability (e.g., for forage growth) during dry seasons. Note that the 80th year is the driest year examined here, so it is notable that the soil under Larch silvopasture experiences the least amount of drying during this year (despite Larch and Sycamore having roughly the same amount of transpiration, see c3). Importantly, this effect seems to persist during the summer season (see b3 in Tables A2, where the soil under Larch is significantly less dry than that under Sycamore or Pine).

This would be consistent with presence of a dense litter layer under Larch which has been observed to persist year-round at Glensaugh. Although the portion of the total evapotranspiration which a litter layer is expected to impact (i.e., soil evaporation) may not be large enough to favour this explanation here. Soils under Larch are also less sandy (by ca. 6-7%), more silty (by ca. 3-4%) and have a higher clay content (by ca. 3-4%) relative to the other sites, which is perhaps more likely to be the main driver of the simulated effect. It is also possible that measurement errors are responsible for the more damped topsoil moisture dynamics observed under Larch (see Figure 1 d) which is subsequently captured by our model as a physical effect. Nevertheless, relative to the other species at this site, Larch shows a notably greater potential in terms of preserving soil moisture under drier conditions. This suggests that the choice of species is likely to be important for soil water availability, particularly for forage growth in silvopastoral systems. Although we have used a bias-corrected future climate data which tends to smooth-out climatic extremes (whether wet or dry), so the significance of such effects under severe drought should be investigated separately.

5.3.3 Implications for river flows

In cases where significant inter-site differences in hydraulic conductivity exist, it is expected to be captured in the bulk soil saturated hydraulic conductivity parameter ($\hat{K}_0$) of our model during calibration. Chandler et al. (2018) measured $\hat{K}_0$ under the Pine and Sycamore silvopasture plots at Glensaugh and compared those to $\hat{K}_0$ measurements under pasture. They found no significant difference between the three sites. They further found that woodland (2500 stems/ha without grazing, also at Glensaugh) showed a significant increase in $\hat{K}_0$ relative to pasture. They concluded that any potential increase in $\hat{K}_0$ under silvopasture at this site is likely countered

https://doi.org/10.5194/egusphere-2024-2258
Preprint. Discussion started: 31 July 2024

by topsoil compaction due to sheep/cattle weights. Our calibrated parameter ranges in Figure 3 show similar distributions for Grass (pasture), Pine, Sycamore as well as for Larch, where $\hat{K}_0$ values, although slightly lower under trees, show significant overlap, providing encouragement that our parameters may have captured soil properties relatively well despite the simple model structure.

The $\hat{p}$ parameter which controls the ease/difficulty with which water can be extracted from the soil (whether by means of flow or evapotranspiration) at different saturation levels, is <1 under Grass, Pine and Sycamore, indicating easier extraction even at lower saturations, but is >1 under Larch indicating the opposite. The observed topsoil moisture dynamics under Larch in Figure 1 d are noticeably more damped compared to the other three sites. As mentioned earlier, the ground under Larch is covered by a dense litter layer year-round, but it also has a higher clay/silt content. So the higher $\hat{p}$ values under Larch could be reflecting either or both of these effects. In any case, it is encouraging that the model seems to be capturing physical effects that impact soil moisture and flow from the soil. Our modelling suggests that pasture to silvopasture conversion at Glensaugh would reduce the total annual outflows (i.e., water yield) from the soil most likely due to greater water loss to evapotranspiration, consistent with experimental (e.g., Soulsby et al. 2017b) and modelling (e.g., Stevenson et al. 2023) studies in the region.

Purely from a process understanding perspective, a reduction in water yield can be considered a positive impact in terms of flood risk mitigation potential, particularly since these reductions seem to persist during the winter seasons (see Table A3 d1) with the evergreen species having a substantially larger impact, likely due to greater transpiration and reductions in near surface flows (Neill et al., 2021). While many numerical studies suggest that significant flood risk mitigation can be possible through increased tree cover at small-scale and under flood-relevant events (e.g., Nisbet & Thomas 2006, Monger et al. 2024), larger scale experimental evidence so far only supports such claims at smaller events not relevant for flooding (Birkinshaw et al., 2014, Fahey & Payne, 2017, Bathurst et al., 2020, Xiao et al., 2022), likely due to the limited effects of trees on transient storage particularly in low-energy, humid environments with shallow soils (Tetzlaff et al., 2007, Soulsby et al., 2017a), which exhibit relatively small dynamic storage Geris et al. (2015b). In these environments soil type (Geris et al., 2015a) and geology (Peskett et al., 2021) are much stronger controls on runoff, especially in large events. Thus, while our results indicate that significant reductions in storm flow may result in smaller events, it seems less likely that significant flood risk mitigation benefits can be derived from silvopastoral practices under flood-relevant events in landscapes that can be represented by Glensaugh.

Similarly, reductions in water yield can be considered a negative impact in terms of river flow regulation during drier periods when river levels depend on groundwater contributions from adjacent soil units. Whether afforestation increases or decreases catchment baseflow is a subject of much debate. Many studies have found increased tree cover to increase baseflow, while many other studies report the opposite (e.g., see the review by Price 2011). The synthesis by Filoso et al. (2017) reflects the lack of consensus; it shows that 63% studies reported a decrease and 37% an increase or no change following afforestation under a wide range of climates and soil/tree types. In our case, during the summer of the driest year examined here (where rainfall decreases by 6% and evapotranspiration increases by 19%, see Table A2 d1, at the 80th year) water yield under Pine silvopasture (although 18% lower relative to pasture) is 7% higher relative to Sycamore silvopasture and 9% higher relative to Larch silvopasture. A 7-9% difference in water yield could be significant for river flow regulation under drought conditions. However, again, because we have used bias-corrected future climate projections it is unclear from our results how much of the 7-9% boost estimated under Pine silvopasture would persist during a severe drought. Nevertheless, according to our results, in locations where river flow/level preservation is important (e.g., for Atlantic Salmon population/migration, Soulsby et al. 2024) yet sensitive to drought, the choice of species should perhaps be made on the basis of the least amount of reduction in water yield (see, e.g., Luo et al. 2024). We suggest that these effects are worth investigating separately, but would likely be important only if the scale of implementation is large.

6 Sources of uncertainty

In agroforestry research there is currently an incommensuratbility between data-availability and system-complexity. We have tried to devise a modelling approach around the data that is likely to be available now (e.g., surface and

https://doi.org/10.5194/egusphere-2024-2258
Preprint. Discussion started: 31 July 2024

above-surface satellite data), but future advances in data collection could improve the situation (e.g., through remote subsurface monitoring) and warrant the use of more complex/complete approaches. Nevertheless uncertainties exist and impact numerical predictions at large. The main sources of uncertainty in our study were as follows. (i) Calculation of carbon stock depends on factors such as bulk density, soil thickness and stoniness of the soil for which we used site average values; (ii) To estimate biomass carbon we used simple allometric equations originally developed for forest stands which tend to have a higher density than 400 stems/ha (and therefore have likely under-predicted biomass at our site); (iii) We used literature values for species-specific maximum tree diameters (e.g., after 200 years) which could have been over- or under-estimations at this site; (iv) In applying RothC we did not distinguish between the different soil layers due to lack of data which could have impacted carbon movement (and therefore estimates) across the soil; (v) By calibrating RSEEP to observed soil moisture data in 2022 and then using those parameters to make past and future predictions, we implicitly assumed that model parameters are independent of calibration data; (vi) There could be significant measurement uncertainty in topsoil moisture and soil carbon data used to calibrated our models which we have not been able to fully quantify; (vii) Our predictions were based on projected climate data which is uncertain; (viii) We assumed that grazing intensity/frequency has been uniform across all silvopasture sites and across time but there was not enough data to support this assumption; and (ix) We have tried to include the main plant-soil-atmospheric interactions in our model, but we have not tested different model structures/complexities to find the best one. More importantly, perhaps, is the interactions of all the different components of uncertainty with one another and how they manifest as the total (yet unknown) level of uncertainty that is inherent in any numerical study. In an attempt to minimise the effects of the total uncertainty we calculated our impact estimates relative to the control site in all years, meaning that any biases that might have resulted from the combination of all uncertainty sources should be controlled for in our 'relative' impact estimates, on which we base our conclusions.

7 Summary, conclusions and future work

We propose RSEEP, a new model to **R**etrieve **S**oil-moisture and **E**stimate **E**cohydrological **P**artitioning, which requires only rainfall, potential evapotranspiration, and surface soil moisture information to run, making it suitable for application in data-limited sites and in conjunction with the available satellite datasets. In a data-rich site, we showed that RSEEP can simulate bulk soil moisture dynamics well under different vegetation types. Further application of our model to different sites would test the generality of this finding. We also coupled RSEEP to RothC soil carbon model to test RothC's sensitivity to soil moisture accounting procedure. A more elaborate soil moisture accounting (than RothC's default) can lead to a 0.08% lower soil carbon estimation per mm reduction in 'effective rainfall' (i.e., rainfall - potential evapotranspiration). Our results suggest to use more elaborate accounting procedures where possible.

We used RSEEP+RothC to simulate the water-carbon dynamics of three different silvopastoral agroforestry systems (all at 400 stems/ha plantation density) in North East Scotland and under the current global emission scenario (RCP6.0). These systems were: (1) evergreen conifer (Scots Pine) silvopasture, (2) deciduous conifer (Hybrid Larch) silvopasture, and (3) deciduous broadleaf (Sycamore) silvopasture. We found that: (i) 40 years after planting trees, total carbon storage (above+below ground) is anywhere between 2-5 times ($\sim$100-250 t/ha) higher under silvopasture than under pasture depending on the choice of species. Deciduous species at this site showed a higher soil carbon turnover potential than evergreen species, but conifer species (whether deciduous or evergreen) outperformed broadleaf species in biomass carbon sequestration. (ii) Larch showed a notably greater potential in terms of preserving soil moisture under drier conditions. The choice of species is therefore likely to be important also for soil water availability under drought, particularly for forage growth in (and therefore longevity of) silvopastoral systems. (iii) Significant reductions in storm flow could be possible during the wet seasons, the amount of which was greatest under the native Scots Pine species. We found Pine to also result in notably smaller reductions in water yield during the dry seasons, making it the overall best choice at this site in terms of river flow regulation in wet and dry conditions. Although these effects are likely to be important only if the scale of implementation is large. (iv) The choice of species was important and should therefore be made on the basis of the ecosystem service priorities/objectives of the site. Finally, we have used a bias-corrected future climate data which tends to smooth-out climatic extremes (whether wet or dry). Examining our scenarios under

https://doi.org/10.5194/egusphere-2024-2258
Preprint. Discussion started: 31 July 2024

drought- and flood-relevant conditions and scales is a logical next step.

8 Code/Data availability

Model codes and data are publicly available to download from Goudarzi (2024).

9 Authors' contributions

SG, CS, JS and JG developed the framework for the study, with input from JLS and AG. SG undertook data processing, model development and application, and drafted the manuscript. JLS collected and processed the soil moisture measurements at Cruickshank Botanic Garden. IA collected and processed the soil moisture measurements at Glensaugh. SR collated and quality checked the soil carbon/tree-biomass data from Glensaugh. SG, CS, JS, JLS, AG, AH, IA and JG discussed the results and contributed to their interpretation and to the evolution of the manuscript to its current point.

10 Competing of Interest

The authors declare no conflicts of interest.

11 Acknowledgements

This work was carried out as part of the FARM TREE project, funded via the UK Natural Environment Research Council (NERC) as part of the UK Research and Innovation (UKRI) Treescapes programme (reference: NE/X004686/1). We thank Matthew Purslow for help with setting up the soil moisture loggers at Glensaugh. We thank Donald Barrie for providing access to the site as well as assistance with building protective cages for the loggers at Glensaugh. We also thank Steven Hancock for providing access to their Glensaugh soil moisture data which was collected as part of a separate project.

References

Abdul-Salam, Y., Ovando, P., & Roberts, D. (2022). Understanding the economic barriers to the adoption of agroforestry: A Real Options analysis. Journal of Environmental Management, 302, 113955. 1

Albergel, C., Rüdiger, C., Pellarin, T., Calvet, J. C., Fritz, N., Froissard, F., ... & Martin, E. (2008). From near-surface to root-zone soil moisture using an exponential filter: an assessment of the method based on in-situ observations and model simulations. Hydrology and Earth System Sciences, 12(6), 1323-1337. 3.1

Bathurst, J. C., Fahey, B., Iroumé, A., & Jones, J. (2020). Forests and floods: using field evidence to reconcile analysis methods. Hydrological Processes, 34(15), 3295-3310. 5.3.3

Bauer, J., Herbst, M., Huisman, J. A., Weihermüller, L., & Vereecken, H. (2008). Sensitivity of simulated soil heterotrophic respiration to temperature and moisture reduction functions. Geoderma, 145(1-2), 17-27. 5.2

Bealde, C. L., Talbot, H., & Jarvis, P. G. (1982). Canopy structure and leaf area index in a mature Scots pine forest. Forestry: An International Journal of Forest Research, 55(2), 105-123. 3.2.2

Beckert, M. R., Smith, P., Lilly, A., & Chapman, S. J. (2015). Soil and tree biomass carbon sequestration potential of silvopastoral and woodland-pasture systems in North East Scotland. Agroforestry Systems, 90, 371-383. 2.2, 5.3.1

https://doi.org/10.5194/egusphere-2024-2258
Preprint. Discussion started: 31 July 2024

Birkinshaw, S. J., Bathurst, J. C., & Robinson, M. (2014). 45 years of non-stationary hydrology over a forest plantation growth cycle, Coalburn catchment, Northern England. Journal of Hydrology, 519, 559-573. 5.3.3

Bunce, R. G. H. (1968). Biomass and production of trees in a mixed deciduous woodland: I. Girth and height as parameters for the estimation of tree dry weight. The Journal of Ecology, 759-775. 3.2.2

Caldwell, M. M., & Richards, J. H. (1989). Hydraulic lift: water efflux from upper roots improves effectiveness of water uptake by deep roots. Oecologia, 79, 1-5. 1

Cardinael, R., Cadisch, G., Gosme, M., Oelbermann, M., & Van Noordwijk, M. (2021). Climate change mitigation and adaptation in agriculture: Why agroforestry should be part of the solution. Agriculture, Ecosystems & Environment, 319, 107555. 1

Cairns, M. A., Brown, S., Helmer, E. H., & Baumgardner, G. A. (1997). Root biomass allocation in the world's upland forests. Oecologia, 111, 1-11. 3.2.2

Chandler, K. R., Stevens, C. J., Binley, A., & Keith, A. M. (2018). Influence of tree species and forest land use on soil hydraulic conductivity and implications for surface runoff generation. Geoderma, 310, 120-127. 2.2, 5.3.3

Chen, J., Kuang, X., & Zheng, C. (2020). An empirical porosity–depth model for Earth's crust. Hydrogeology Journal, 28(7), 2331-2339. 3.1.1

Coleman, K., & Jenkinson, D. S. (2014). RothC-A model for the turnover of carbon in soil Model description and users guide (Windows version)(updated June 2014). 3.2.1, 3.2.1

Dawson, T. E. (1993). Hydraulic lift and water use by plants: implications for water balance, performance and plant-plant interactions. Oecologia, 95, 565-574. 1

Dawson, T. E. (1996). Determining water use by trees and forests from isotopic, energy balance and transpiration analyses: the roles of tree size and hydraulic lift. Tree physiology, 16(1-2), 263-272. 1

Demand, D., Blume, T., & Weiler, M. (2019). Spatio-temporal relevance and controls of preferential flow at the landscape scale. Hydrology and Earth System Sciences, 23(11), 4869-4889. 5.1

Den Herder, M., Moreno, G., Mosquera-Losada, R. M., Palma, J. H., Sidiropoulou, A., Freijanes, J. J. S., ... & Burgess, P. J. (2017). Current extent and stratification of agroforestry in the European Union. Agriculture, Ecosystems & Environment, 241, 121-132. 1

Duguma, L. A., Minang, P. A., & van Noordwijk, M. (2014). Climate change mitigation and adaptation in the land use sector: from complementarity to synergy. Environmental management, 54, 420-432. 1

Duguma, L. A., Wambugu, S. W., Minang, P. A., & Van Noordwijk, M. (2014). A systematic analysis of enabling conditions for synergy between climate change mitigation and adaptation measures in developing countries. Environmental science policy, 42, 138-148. 1

Duethmann, D., Smith, A., Soulsby, C., Kleine, L., Wagner, W., Hahn, S., & Tetzlaff, D. (2022). Evaluating satellite-derived soil moisture data for improving the internal consistency of process-based ecohydrological modelling. Journal of hydrology, 614, 128462. 1

Elsherif, A., Gaulton, R., Mills, J. P., & Sharaf El Din, E. (2023). Measuring Forest Canopy Water Mass in Three Dimensions Using Terrestrial Laser Scanning. The International Archives of the Photogrammetry, Remote Sensing and Spatial Information Sciences, 48, 721-726. 3.2.2

Emerman, S. H., & Dawson, T. E. (1996). Hydraulic lift and its influence on the water content of the rhizosphere: an example from sugar maple, Acer saccharum. Oecologia, 108, 273-278. 1

https://doi.org/10.5194/egusphere-2024-2258
Preprint. Discussion started: 31 July 2024

Fahey, B., & Payne, J. (2017). The Glendhu experimental catchment study, upland east Otago, New Zealand: 34 years of hydrological observations on the afforestation of tussock grasslands. Hydrological Processes, 31(16), 2921-2934. 5.3.3

Falloon, P., & Betts, R. (2010). Climate impacts on European agriculture and water management in the context of adaptation and mitigation—the importance of an integrated approach. Science of the total environment, 408(23), 5667-5687. 1

Falloon, P., Jones, C. D., Ades, M., & Paul, K. (2011). Direct soil moisture controls of future global soil carbon changes: An important source of uncertainty. Global Biogeochemical Cycles, 25(3). 1, 5.2

Finér, L., Helmisaari, H. S., Lõhmus, K., Majdi, H., Brunner, I., Børja, I., ... & Vanguelova, E. (2007). Variation in fine root biomass of three European tree species: Beech (Fagus sylvatica L.), Norway spruce (Picea abies L. Karst.), and Scots pine (Pinus sylvestris L.). Plant Biosystems, 141(3), 394-405. 5.3.1

Filoso, S., Bezerra, M. O., Weiss, K. C., & Palmer, M. A. (2017). Impacts of forest restoration on water yield: A systematic review. PloS one, 12(8), e0183210. 5.3.3

García de Jalón, S., Burgess, P. J., Graves, A., Moreno, G., McAdam, J., Pottier, E., ... & Vityi, A. (2018). How is agroforestry perceived in Europe? An assessment of positive and negative aspects by stakeholders. Agroforestry Systems, 92, 829-848. 1

Gardner, W. R. (1983). Soil properties and efficient water use: an overview. Limitations to efficient water use in crop production, 45-64. 5.1

Gentine, P., Green, J. K., Guérin, M., Humphrey, V., Seneviratne, S. I., Zhang, Y., & Zhou, S. (2019). Coupling between the terrestrial carbon and water cycles—a review. Environmental Research Letters, 14(8), 083003. 1

Geris, J., Tetzlaff, D., McDonnell, J., & Soulsby, C. (2015). The relative role of soil type and tree cover on water storage and transmission in northern headwater catchments. Hydrological Processes, 29(7), 1844-1860. 5.3.3

Geris, J., Tetzlaff, D., & Soulsby, C. (2015). Resistance and resilience to droughts: hydropedological controls on catchment storage and run-off response. Hydrological Processes, 29(21), 4579-4593. 5.3.3

Gottschalk, P., Smith, J. U., Wattenbach, M., Bellarby, J., Stehfest, E., Arnell, N., ... & Smith, P. (2012). How will organic carbon stocks in mineral soils evolve under future climate? Global projections using RothC for a range of climate change scenarios. Biogeosciences, 9(8), 3151-3171. 1

Goudarzi, S., (2024). RSEEP: A model to Retrieve Soil-moisture and Estimate Ecohydrological Partitioning [Software and Data]. DOIhttps://zenodo.org/doi/10.5281/zenodo.12781754. 8

Gower, S. T., & Richards, J. H. (1990). Larches: deciduous conifers in an evergreen world. BioScience, 40(11), 818-826. 3.2.2

Guo, L. B., & Gifford, R. M. (2002). Soil carbon stocks and land use change: a meta analysis. Global change biology, 8(4), 345-360. 5.3.1

Hall, S. J., & Bunce, R. G. (2011). Mature trees as keystone structures in Holarctic ecosystems–a quantitative species comparison in a northern English park. Plant Ecology Diversity, 4(2-3), 243-250. 3.2.2

Hübner, R., Kühnel, A., Lu, J., Dettmann, H., Wang, W., & Wiesmeier, M. (2021). Soil carbon sequestration by agroforestry systems in China: A meta-analysis. Agriculture, Ecosystems & Environment, 315, 107437. 1

Lee, H., Calvin, K., Dasgupta, D., Krinner, G., Mukherji, A., Thorne, P., ... & Ruane, A. C. (2024). Climate change 2023 synthesis report summary for policymakers. CLIMATE CHANGE 2023 Synthesis Report: Summary for Policymakers. 1

https://doi.org/10.5194/egusphere-2024-2258
Preprint. Discussion started: 31 July 2024

Iorgulescu, I., & Musy, A. (1997). Generalization of TOPMODEL for a power law transmissivity profile. Hydrological processes, 11(9), 1353-1355. 3.1.1

Jarvis, N. J., Zavattaro, L., Rajkai, K., Reynolds, W. D., Olsen, P. A., McGechan, M., ... & Jacques, D. (2002). Indirect estimation of near-saturated hydraulic conductivity from readily available soil information. Geoderma, 108(1-2), 1-17. 3.1.1

Jebari, A., Álvaro-Fuentes, J., Pardo, G., Almagro, M., & Del Prado, A. (2021). Estimating soil organic carbon changes in managed temperate moist grasslands with RothC. PLoS One, 16(8), e0256219. 1

Knoben, W. J., Freer, J. E., & Woods, R. A. (2019). Inherent benchmark or not? Comparing Nash–Sutcliffe and Kling–Gupta efficiency scores. Hydrology and Earth System Sciences, 23(10), 4323-4331. 4.1

Kostov, K. G., & Jackson, T. J. (1993, August). Estimating profile soil moisture from surface-layer measurements: A review. In Ground Sensing (Vol. 1941, pp. 125-136). SPIE. 3.1

Kozak, J. A., Ahuja, L. R., Green, T. R., & Ma, L. (2007). Modelling crop canopy and residue rainfall interception effects on soil hydrological components for semi-arid agriculture. Hydrological Processes: An International Journal, 21(2), 229-241. 3.1.1

Lal, R., Smith, P., Jungkunst, H. F., Mitsch, W. J., Lehmann, J., Nair, P. R., ... & Ravindranath, N. H. (2018). The carbon sequestration potential of terrestrial ecosystems. Journal of soil and water conservation, 73(6), 145A-152A. 5.3.1

Larsson-Stern, M. (2012). Larch in commercial forestry: A literature review to help clarify the potential of hybrid larch (Larix× eurolepis Henry) in Southern Sweden. Southern Swedish Forest Research Centre Alnarp, Sweden. 3.2.2

Li, Z. L., Leng, P., Zhou, C., Chen, K. S., Zhou, F. C., & Shang, G. F. (2021). Soil moisture retrieval from remote sensing measurements: Current knowledge and directions for the future. Earth-Science Reviews, 218, 103673. 1

Li, M., Sun, H., & Zhao, R. (2023). A Review of Root Zone Soil Moisture Estimation Methods Based on Remote Sensing. Remote Sensing, 15(22), 5361. 1

Lilly, A., Chapman, S. J., Perez-Fernandez, E., & Potts, J. (2016). Changes to C stocks in Scottish soils due to afforestation. Contract Report to Forestry Commission. 5.3.1

Liu, Y., & Yang, Y. (2022). Advances in the quality of global soil moisture products: a review. Remote Sensing, 14(15), 3741. 1

Lim, M. T., & Cousens, J. E. (1986). The internal transfer of nutrients in a Scots pine stand I. Biomass components, current growth and their nutrient content. Forestry: An International Journal of Forest Research, 59(1), 1-16. 3.2.2

Liste, H. H., & White, J. C. (2008). Plant hydraulic lift of soil water–implications for crop production and land restoration. Plant and Soil, 313, 1-17. 1

Luo, S., Tetzlaff, D., Smith, A., & Soulsby, C. (2024). Assessing impacts of alternative land use strategies on water partitioning, storage and ages in drought-sensitive lowland catchments using tracer-aided ecohydrological modelling. Hydrological Processes, 38(4), e15126. 5.3.3

Menichetti, L., Kätterer, T., & Bolinder, M. A. (2020). A Bayesian modeling framework for estimating equilibrium soil organic C sequestration in agroforestry systems. Agriculture, ecosystems & environment, 303, 107118. 1

https://doi.org/10.5194/egusphere-2024-2258
Preprint. Discussion started: 31 July 2024

Mishra, V., Ellenburg, W. L., Markert, K. N., & Limaye, A. S. (2020). Performance evaluation of soil moisture profile estimation through entropy-based and exponential filter models. Hydrological Sciences Journal, 65(6), 1036-1048. 1, 3.1

Monger, F., Spracklen, D. V., Kirkby, M. J., & Willis, T. (2024). Investigating the impact of woodland placement and percentage cover on flood peaks in an upland catchment using spatially distributed TOPMODEL. Journal of Flood Risk Management, e12977. 5.3.3

Mosquera-Losada, M. R., Santiago-Freijanes, J. J., Rois-DíAz, M., Moreno, G., den Herder, M., Aldrey-Vázquez, J. A., ... & Rigueiro-Rodríguez, A. (2018). Agroforestry in Europe: A land management policy tool to combat climate change. Land use policy, 78, 603-613. 1

Moyano, F. E., Vasilyeva, N., Bouckaert, L., Cook, F., Craine, J., Curiel Yuste, J., ... & Chenu, C. (2012). The moisture response of soil heterotrophic respiration: interaction with soil properties. Biogeosciences, 9(3), 1173-1182. 1

Nair, P. R., Kumar, B. M., & Nair, V. D. (2021). An introduction to agroforestry: four decades of scientific developments (pp. 3-20). Cham: Springer. 1

Neill, A. J., Birkel, C., Maneta, M. P., Tetzlaff, D., & Soulsby, C. (2021). Structural changes to forests during regeneration affect water flux partitioning, water ages and hydrological connectivity: Insights from tracer-aided ecohydrological modelling. Hydrology and Earth System Sciences, 25(9), 4861-4886. 5.3.3

Noordwijk, M. V., Hoang, M. H., Neufeldt, H., Öborn, I., & Yatich, T. (2011). How trees and people can co-adapt to climate change: reducing vulnerability in multifunctional landscapes (pp. xi+-133). 1

Nisbet, T. R., & Thomas, H. (2006). The role of woodland in flood control: a landscape perspective. Forest Research. 5.3.3

Nwaigbo, L. C. (1996). Spatial variation of tree growth and site factors in a silvopastoral system in northeast Scotland (Doctoral dissertation, University of Aberdeen). 2.2

Pan, X., Kornelsen, K. C., & Coulibaly, P. (2017). Estimating root zone soil moisture at continental scale using neural networks. JAWRA Journal of the American Water Resources Association, 53(1), 220-237. 3.1

Peskett, L. M., Heal, K. V., MacDonald, A. M., Black, A. R., & McDonnell, J. J. (2021). Tracers reveal limited influence of plantation forests on surface runoff in a UK natural flood management catchment. Journal of Hydrology: Regional Studies, 36, 100834. 5.3.3

Price, K. (2011). Effects of watershed topography, soils, land use, and climate on baseflow hydrology in humid regions: A review. Progress in physical geography, 35(4), 465-492. 5.3.3

Qin, M., Giménez, D., & Miskewitz, R. (2018). Temporal dynamics of subsurface soil water content estimated from surface measurement using wavelet transform. Journal of hydrology, 563, 834-850. 3.1

Robinson, D. A., Thomas, A., Reinsch, S., Lebron, I., Feeney, C. J., Maskell, L. C., ... & Cosby, B. J. (2022). Analytical modelling of soil porosity and bulk density across the soil organic matter and land-use continuum. Scientific reports, 12(1), 7085. 3.1.1

Ražauskaitė, R., Vanguelova, E., Cornulier, T., Smith, P., Randle, T., & Smith, J. U. (2020). A new approach using modeling to interpret measured changes in soil organic carbon in forests; the case of a 200 year pine chronosequence on a podzolic soil in Scotland. Frontiers in Environmental Science, 8, 527549. 3.2.1

Robinson, E. L., Huntingford, C., Semeena, V. S., & Bullock, J. M. (2023). CHESS-SCAPE: High resolution future projections of multiple climate scenarios for the United Kingdom derived from downscaled UKCP18 regional climate model output. Earth System Science Data Discussions, 2023, 1-51. 2.2

https://doi.org/10.5194/egusphere-2024-2258
Preprint. Discussion started: 31 July 2024

Rutgers, M., Orgiazzi, A., Gardi, C., Römbke, J., Jänsch, S., Keith, A. M., ... & De Zwart, D. (2016). Mapping earthworm communities in Europe. Applied Soil Ecology, 97, 98-111. 5.1

Sadeghi, M., Tabatabaeenejad, A., Tuller, M., Moghaddam, M., & Jones, S. B. (2016). Advancing NASA's AirMOSS P-band radar root zone soil moisture retrieval algorithm via incorporation of Richards' equation. Remote Sensing, 9(1), 17. 3.1

Schelhaas, M. J., Hengeveld, G. M., Heidema, N., Thürig, E., Rohner, B., Vacchiano, G., ... & Nabuurs, G. J. (2018). Species-specific, pan-European diameter increment models based on data of 2.3 million trees. Forest Ecosystems, 5, 1-19. 3.2.2

Simon, J. C., and G. Lemaire. Tillering and leaf area index in grasses in the vegetative phase. Grass and Forage Science 42.4 (1987): 373-380. 3.2.2

Singh, V. P. (2010). Entropy theory for movement of moisture in soils. Water resources research, 46(3). 3.1

Smith, J., Gottschalk, P., Bellarby, J., Chapman, S., Lilly, A., Towers, W., ... & Smith, P. (2010). Estimating changes in Scottish soil carbon stocks using ECOSSE. I. Model description and uncertainties. Climate Research, 45, 179-192. 3.2.1

Smith, J., Pearce, B. D., & Wolfe, M. S. (2012). A European perspective for developing modern multifunctional agroforestry systems for sustainable intensification. Renewable Agriculture and Food Systems, 27(4), 323-332. 1

Smith, J., Pearce, B. D., & Wolfe, M. S. (2013). Reconciling productivity with protection of the environment: Is temperate agroforestry the answer?. Renewable Agriculture and Food Systems, 28(1), 80-92. 1

Smith, A., Tetzlaff, D., Kleine, L., Maneta, M., & Soulsby, C. (2021). Quantifying the effects of land use and model scale on water partitioning and water ages using tracer-aided ecohydrological models. Hydrology and Earth System Sciences, 25(4), 2239-2259. 1

Sollen-Norrlin, M., Ghaley, B. B., & Rintoul, N. L. J. (2020). Agroforestry benefits and challenges for adoption in Europe and beyond. Sustainability, 12(17), 7001. 1

Soulsby, C., Dick, J., Scheliga, B., & Tetzlaff, D. (2017). Taming the flood-How far can we go with trees?. Hydrological Processes, 31(17). 5.3.3

Soulsby, C., Braun, H., Sprenger, M., Weiler, M., & Tetzlaff, D. (2017). Influence of forest and shrub canopies on precipitation partitioning and isotopic signatures. Hydrological Processes, 31(24), 4282-4296. 5.3.2, 5.3.3

Soulsby, C., Youngson, A., & Webb, J. (2024). The ecohydrology of rewilding: A pressing need for evidence in the restoration of upland Atlantic salmon streams. Hydrological Processes, 38(5), e15142. 5.3.3

Srivastava, S. K., Yograjan, N., Jayaraman, V., Rao, P. N., & Chandrasekhar, M. G. (1997). On the relationship between ERS-1 SAR/backscatter and surface/sub-surface soil moisture variations in vertisols. Acta Astronautica, 40(10), 693-699. 3.1

Stevenson, J. L., Birkel, C., Comte, J. C., Tetzlaff, D., Marx, C., Neill, A., ... & Soulsby, C. (2023). Quantifying heterogeneity in ecohydrological partitioning in urban green spaces through the integration of empirical and modelling approaches. Environmental Monitoring and Assessment, 195(4), 468. 2.1, 5.3.2, 5.3.3

Nan, S., Yazhou, L., & Meng, L. (2012). The influences of planting density to aboveground biomass distribution of hybrid larch. 3.2.2

Tetzlaff, D., Malcolm, I. A., & Soulsby, C. (2007). Influence of forestry, environmental change and climatic variability on the hydrology, hydrochemistry and residence times of upland catchments. Journal of Hydrology, 346(3-4), 93-111. 5.3.3

https://doi.org/10.5194/egusphere-2024-2258
Preprint. Discussion started: 31 July 2024

Tobin, K. J., Torres, R., Crow, W. T., & Bennett, M. E. (2017). Multi-decadal analysis of root-zone soil moisture applying the exponential filter across CONUS. Hydrology and Earth System Sciences, 21(9), 4403-4417. 3.1

Upson, M. A., Burgess, P. J., & Morison, J. I. L. (2016). Soil carbon changes after establishing woodland and agroforestry trees in a grazed pasture. Geoderma, 283, 10-20. 5.3.1

van Dam, J. C., & Feddes, R. A. (2000). Numerical simulation of infiltration, evaporation and shallow groundwater levels with the Richards equation. Journal of hydrology, 233(1-4), 72-85. 3.1

van Dijk, A. I. J. M., & Bruijnzeel, L. A. (2001). Modelling rainfall interception by vegetation of variable density using an adapted analytical model. Part 1. Model description. Journal of Hydrology, 247(3-4), 230-238. 3.1.1, 3.1.1

Vesterdal, L., Elberling, B., Christiansen, J. R., Callesen, I., & Schmidt, I. K. (2012). Soil respiration and rates of soil carbon turnover differ among six common European tree species. Forest Ecology and Management, 264, 185-196. 5.3.1

Wang, Y., Zhao, H., Fan, J., Wang, C., Ji, X., Jin, D., | Chen, J. (2023). A Review of Earth's Surface Soil Moisture Retrieval Models via Remote Sensing. Water, 15(21), 3757. 1

Xiao, L., Robinson, M., & O'Connor, M. (2022). Woodland's role in natural flood management: Evidence from catchment studies in Britain and Ireland. Science of the Total Environment, 813, 151877. 5.3.3

https://doi.org/10.5194/egusphere-2024-2258
Preprint. Discussion started: 31 July 2024

12 Appendix: the full range of model predictions

Table A1: The annual environmental impacts of converting pasture (P) to silvopasture (SP) at Glensaugh 20, 40 and 80 years after conversion. Green values=increase; red values= decrease; display format= median%(5th percentile: 95th percentile) of 160,000 model predictions. All percentages are relative to their respective reference value at '+0 yrs' which represents the pasture without trees base-case at time $t = 0$, i.e., in 1987.

P : Pasture **SP:** Silvopasture	**+0 yrs**	**+20 yrs**	**+40 yrs**	**+80 yrs**	
		Climate			(a)
R	1059 mm/yr	+15% (14:16)	+21% (15:31)	+12% (11:13)	
P_{ETg}	331 mm/yr	+4% (3:5)	+7% (7:8)	+19% (18:19)	
R - P_{ETg}	729 mm/yr	+11% (10:35)	+27% (2:36)	+7% (2:15)	
		Storage dynamics			
		Soil carbon/ha			(b1)
P ----> Pine SP		-14% (-21:-7)	+66% (50:81)	+208% (189:246)	
P ----> Larch SP	**52 t**	+4% (-3:12)	+107% (88:119)	+286% (264:329)	
P ----> Syca. SP		-12% (-18:-4)	+70% (52:82)	+222% (206:258)	
		Soil + biomass carbon/ha			(b2)
P ----> Pine SP		+65% (59:71)	+498% (482:512)	+1515% (1497:1551)	
P ----> Larch SP	**52 t**	+87% (80:94)	+517% (499:529)	+1599% (1579:1640)	
P ----> Syca. SP		+13% (7:20)	+216% (198:228)	+844% (828:877)	
		Storage deficit (annual average)			(b3)
P ----> Pine SP		+26% (-67:139)	+88% (14:177)	+230% (90:399)	
P ----> Larch SP	**17 mm**	+19% (-29:124)	+65% (5:119)	+113% (16:215)	
P ----> Syca. SP		+17% (-48:124)	+59% (-11:120)	+159% (33:296)	
		Green water fluxes			
		Canopy evaporation			(c1)
P ----> Pine SP		+26% (22:34)	+57% (51:67)	+83% (75:98)	
P ----> Larch SP	**66 [mm/yr]**	+17% (12:25)	+38% (28:44)	+67% (54:87)	
P ----> Syca. SP		+11% (7:18)	+28% (19:33)	+55% (42:73)	
		Soil evaporation			(c2)
P ----> Pine SP		-16% (-25:-7)	-42% (-49:-35)	-71% (-82:-62)	
P ----> Larch SP	**25 [mm/yr]**	-14% (-21:-8)	-35% (-42:-28)	-65% (-76:-58)	
P ----> Syca. SP		-9% (-17:-1)	-26% (-34:-19)	-59% (-69:-51)	
		Transpiration			(c3)
P ----> Pine SP		+62% (36:93)	+141% (114:170)	+221% (176:286)	
P ----> Larch SP	**83 [mm/yr]**	+50% (31:73)	+103% (79:131)	+153% (114:200)	
P ----> Syca. SP		+36% (15:62)	+87% (61:119)	+167% (128:222)	
		Total ET			(c4)
P ----> Pine SP		+38% (25:52)	+82% (67:97)	+127% (100:158)	
P ----> Larch SP	**174 [mm/yr]**	+29% (18:38)	+57% (46:72)	+89% (65:114)	
P ----> Syca. SP		+20% (9:32)	+47% (36:64)	+92% (67:119)	
		Blue water fluxes			
		Annual water yield			(d1)
P ----> Pine SP		-6% (-27:14)	-13% (-42:13)	-20% (-30:-11)	
P ----> Larch SP	**885 [mm/yr]**	-5% (-25:15)	-9% (-38:17)	-15% (-25:-5)	
P ----> Syca. SP		-4% (-24:16)	-8% (-37:18)	-15% (-25:-6)	

* soil thickness = 0.5 m

https://doi.org/10.5194/egusphere-2024-2258
Preprint. Discussion started: 31 July 2024

Table A2: The summer-time (Jun+Jul+Aug) environmental impacts of converting pasture (P) to silvopasture (SP) at Glensaugh 20, 40 and 80 years after conversion. Green values=increase; red values= decrease; display format= median%(5th percentile:95th percentile) of 160,000 model predictions. All percentages are relative to their respective reference value at '+0 yrs' which represents the pasture without trees base-case at time $t = 0$, i.e., in 1987.

P : Pasture **SP:** Silvopasture	**+0 yrs**	**+20 yrs**		**+40 yrs**		**+80 yrs**		
		Climate						(a)
R	254 mm/JJA	-3%	(-9:12)	+18%	(-7:40)	-6%	(-44:5)	
P_{ETg}	128 mm/JJA	+3%	(-7:17)	+8%	(-4:17)	+19%	(8:31)	
R - P_{ETg}	126 mm/JJA	-11%	(-23:18)	+30%	(-35:87)	-24%	(-131:2)	
		Storage dynamics						
		Soil carbon/ha						(b1)
P ----> Pine SP		-16%	(-22:-9)	+63%	(46:78)	+202%	(184:241)	
P ----> Larch SP	**52 t**	+2%	(-4:10)	+102%	(83:115)	+279%	(257:322)	
P ----> Syca. SP		-13%	(-20:-6)	+66%	(48:79)	+215%	(199:252)	
		Soil + biomass carbon/ha						(b2)
P ----> Pine SP		+64%	(58:70)	+494%	(479:509)	+1509%	(1491:1546)	
P ----> Larch SP	**52 t**	+85%	(79:92)	+513%	(495:525)	+1592%	(1572:1634)	
P ----> Syca. SP		+11%	(5:19)	+212%	(195:224)	+837%	(822:871)	
		storage deficit (summer average)						(b3)
P ----> Pine SP		+21%	(-170:289)	+87%	(-48:293)	+271%	(-33:881)	
P ----> Larch SP	**23 mm**	+26%	(-125:251)	+73%	(-48:219)	+143%	(-153:587)	
P ----> Syca. SP		+19%	(-149:254)	+59%	(-74:216)	+221%	(-99:765)	
		Green water fluxes						
		Canopy evaporation						(c1)
P ----> Pine SP		+15%	(3:28)	+32%	(13:48)	+34%	(3:80)	
P ----> Larch SP	**20 [mm/JJA]**	+25%	(13:44)	+56%	(44:67)	+101%	(70:156)	
P ----> Syca. SP		+17%	(5:33)	+40%	(30:52)	+82%	(52:132)	
		Soil evaporation						(c2)
P ----> Pine SP		-16%	(-35:4)	-38%	(-52:-22)	-61%	(-77:-44)	
P ----> Larch SP	**9 [mm/JJA]**	-17%	(-30:-5)	-45%	(-51:-25)	-77%	(-85:-59)	
P ----> Syca. SP		-12%	(-27:5)	-35%	(-42:-15)	-74%	(-82:-57)	
		Transpiration						(c3)
P ----> Pine SP		+47%	(9:95)	+109%	(60:148)	+164%	(106:229)	
P ----> Larch SP	**40 [mm/JJA]**	+60%	(24:89)	+113%	(70:156)	+139%	(93:188)	
P ----> Syca. SP		+41%	(3:80)	+100%	(49:145)	+173%	(119:235)	
		Total ET						(c4)
P ----> Pine SP		+30%	(7:56)	+65%	(41:87)	+95%	(62:130)	
P ----> Larch SP	**69 [mm/JJA]**	+38%	(19:54)	+75%	(52:100)	+100%	(68:135)	
P ----> Syca. SP		+27%	(5:49)	+63%	(37:91)	+114%	(82:148)	
		Blue water fluxes						
		Summer water yield						(d1)
P ----> Pine SP		-9%	(-27:27)	-21%	(-89:46)	-18%	(-48:31)	
P ----> Larch SP	**207 [mm/JJA]**	-7%	(-27:27)	-18%	(-92:48)	-27%	(-64:22)	
P ----> Syca. SP		-5%	(-25:30)	-15%	(-89:52)	-25%	(-61:24)	

* soil thickness = 0.5 m
** JJA= Jun + Jul + Aug

https://doi.org/10.5194/egusphere-2024-2258
Preprint. Discussion started: 31 July 2024

Table A3: The winter-time (Dec+Jan+Feb) environmental impacts of converting pasture (P) to silvopasture (SP) at Glensaugh 20, 40 and 80 years after conversion. Green values=increase; red values= decrease; display format= median%(5th percentile:95th percentile) of 160,000 model predictions. All percentages are relative to their respective reference value at '+0 yrs' which represents the pasture without trees base-case at time $t = 0$, i.e., in 1987.

P : Pasture **SP:** Silvopasture	**+0 yrs**	**+20 yrs**		**+40 yrs**		**+80 yrs**		
		Climate						(a)
R	282 mm/DJF	+9%	(1:32)	+14%	(-2:18)	+12%	(-7:53)	
P_{ETg}	45 mm/DJF	+8%	(1:16)	+9%	(3:21)	+19%	(2:29)	
R - P_{ETg}	234 mm/DJF	+9%	(1:37)	+14%	(-3:20)	+11%	(-11:58)	
		Storage dynamics						
		Soil carbon/ha						(b1)
P ----> Pine SP		-14%	(-21:-7)	+68%	(51:83)	+211%	(193:250)	
P ----> Larch SP	**52 t**	+4%	(-2:12)	+108%	(89:121)	+290%	(268:333)	
P ----> Syca. SP		-12%	(-18:-4)	+71%	(53:84)	+226%	(209:261)	
		Soil + biomass carbon/ha						(b2)
P ----> Pine SP		+65%	(59:72)	+499%	(483:514)	+1518%	(1500:1554)	
P ----> Larch SP	**52 t**	+87%	(81:95)	+519%	(501:531)	+1603%	(1583:1644)	
P ----> Syca. SP		+13%	(7:20)	+217%	(200:229)	+847%	(831:880)	
		Storage deficit (winter average)						(b3)
P ----> Pine SP		+22%	(-48:90)	+70%	(3:133)	+90%	(-13:408)	
P ----> Larch SP	**6 mm**	+14%	(-39:72)	+35%	(-38:92)	+74%	(-14:181)	
P ----> Syca. SP		+12%	(-45:72)	+29%	(-45:86)	+71%	(-18:185)	
		Green water fluxes						
		Canopy evaporation						(c1)
P ----> Pine SP		+35%	(30:42)	+76%	(61:90)	+119%	(102:149)	
P ----> Larch SP	**14 [mm/DJF]**	+9%	(4:15)	+19%	(8:27)	+31%	(19:46)	
P ----> Syca. SP		+6%	(1:12)	+14%	(4:22)	+26%	(14:40)	
		Soil evaporation						(c2)
P ----> Pine SP		-13%	(-30:0)	-35%	(-59:-24)	-66%	(-87:-42)	
P ----> Larch SP	**2 [mm/DJF]**	-7%	(-24:7)	-18%	(-38:-2)	-32%	(-57:-6)	
P ----> Syca. SP		-5%	(-21:9)	-13%	(-33:3)	-26%	(-52:2)	
		Transpiration						(c3)
P ----> Pine SP		+73%	(49:98)	+159%	(131:199)	+256%	(168:353)	
P ----> Larch SP	**7 [mm/DJF]**	+33%	(12:54)	+64%	(56:103)	+131%	(76:202)	
P ----> Syca. SP		+23%	(4:42)	+49%	(38:83)	+114%	(59:178)	
		Total ET						(c4)
P ----> Pine SP		+43%	(30:58)	+90%	(78:115)	+143%	(106:189)	
P ----> Larch SP	**23 [mm/DJF]**	+15%	(5:28)	+31%	(21:49)	+59%	(30:90)	
P ----> Syca. SP		+11%	(0:23)	+24%	(12:40)	+50%	(23:80)	
		Blue water fluxes						
		Winter water yield						(d1)
P ----> Pine SP		-4%	(-39:31)	-9%	(-30:12)	-13%	(-76:43)	
P ----> Larch SP	**260 [mm/DJF]**	-3%	(-38:33)	-3%	(-26:16)	-5%	(-64:56)	
P ----> Syca. SP		-2%	(-38:34)	-2%	(-25:17)	-5%	(-64:57)	

* soil thickness = 0.5 m
**DJD= Dec + Jan + Feb